Czech Technical University in Prague
Faculty of Electrical Engineering
Department of Measurement

Resonant and Transmission Properties of a Periodic Binary Acoustic Waveguide

Bachelor's thesis

Matěj Nešpor

Supervisor: prof. Dr. Ing. Michal Bednařík
Study Programme: Cybernetics and Robotics

May 2024

BACHELOR‘S THESIS ASSIGNMENT

I. Personal and study details

Student's name: **Nešpor Matěj** Personal ID number: **507228**

Faculty / Institute: **Faculty of Electrical Engineering**

Department / Institute: **Department of Measurement**

Study program: **Cybernetics and Robotics**

II. Bachelor’s thesis details

Bachelor’s thesis title in English:

Resonant and transmission properties of a periodic binary acoustic waveguide

Bachelor’s thesis title in Czech:

Rezonanční a přenosové vlastnosti periodického binárního akustického vlnovodu

Guidelines:

Perform an analysis of the resonant and transmission properties of a periodic binary acoustic waveguide (with stepwise changes in the cross-sectional area) using the Transfer Matrix Method (TMM) and the Su-Schrieffer-Heeger (SSH) model. Focus on investigating both bulk modes and edge modes (under what conditions edge modes can be excited) depending on the termination of the finite waveguide and the ratio of cross-sectional areas of its individual elements. In describing the behavior of the investigated waveguide, rely on Bloch's theory and employ concepts and methods used in acoustic topology. Compare the advantages and disadvantages of approaches based on the TMM and SSH model. Implement calculations using mathematical software such as Maple or, if necessary, programs created for this purpose in the Python language.

Bibliography / sources:

[1] A. Coutant, A. Sivadon, L. Zheng, V. Achilleos, O. Richoux, G. Thepcharis, V. Paneux: Acoustic Su-Schrieffer-Heeger lattice: Direct mapping of acoustic waveguides to the Su-Schrieffer-Heeger model, Phys. Rev. B, 103, 224309 (2021).
[2] P. Markoš, C. M. Soukoulis: Wave propagation – From Electrons to Photonic Crystals and Left-Handed Materials, Princeton University Press (2008).
[3] D. J. Griffiths and C. A. Steinke: Waves in locally periodic media, Am. J. Phys., 69 (2), 137-154 (2001).
[4] J. K. Asbóth, L. Oroszlány, A. Pályi: A Short Cource on Topological Insulaters - Band-structure topology and edge states in one and two dimensions, Springer (2015).

Name and workplace of bachelor’s thesis supervisor:

prof. Dr. Ing. Michal Bednařík Department of Physics FEE

Name and workplace of second bachelor’s thesis supervisor or consultant:

Date of bachelor’s thesis assignment: **01.02.2024** Deadline for bachelor thesis submission: **24.05.2024**

Assignment valid until:
by the end of summer semester 2024/2025

prof. Dr. Ing. Michal Bednařík	Head of department's signature	prof. Mgr. Petr Páta, Ph.D.
Supervisor's signature		Dean's signature

III. Assignment receipt

The student acknowledges that the bachelor’s thesis is an individual work. The student must produce his thesis without the assistance of others, with the exception of provided consultations. Within the bachelor’s thesis, the author must state the names of consultants and include a list of references.

. | Date of assignment receipt

Student’s signature

Acknowledgements

I would like to express my deepest gratitude and appreciation to my supervisor, Michal Bednařík, for his invaluable guidance, support, and encouragement throughout this thesis. His mentorship has inspired me not only in the academic realm but also beyond it.

Declaration

I hereby declare that I have independently completed the thesis presented and that all sources utilized have been cited in accordance with the Methodological Instructions governing the ethical principles of academic thesis writing.

In Prague, on May 4, 2024

.....
Matěj Nešpor

Abstract

This bachelor's thesis deals with the resonance and transmission properties of a periodic binary acoustic waveguide characterized by step changes of its cross section. The investigation is carried out using two analytical methods: the Transfer Matrix Method (TMM) and the Su-Schrieffer-Heeger (SSH) Model. The study focuses on both bulk and edge modes, with particular emphasis on the conditions under which the edge modes can be observed. This includes an analysis of the effect of different terminations of the finite waveguide and different aspect ratios of the cross-sectional areas of its individual elements. The thesis compares the advantages and disadvantages of the TMM and the SSH model in order to determine which of the methods provides more telling results about the properties of the waveguide. Selected calculations and symbolic derivations are performed using Maple software and are attached to this thesis.

Keywords:
Su-Schrieffer-Heeger Model; Transfer Matrix Method; Locally Periodic Structures; Bulk Modes; Edge Modes; Band Gap; Bloch-Floquet Theorem

Abstrakt

Tato bakalářská práce se zabývá rezonančními a přenosovými vlastnostmi periodického binárního akustického vlnovodu charakterizovaného skokovými změnami jeho průřezu. Vyšetřování vlastností je prováděno pomocí dvou analytických metod: metody matice přechodu (TMM) a Su-Schrieffer-Heegerova (SSH) modelu. Rozbor se zaměřuje na objemové i okrajové módy, přičemž zvláštní důraz je kladen na podmínky, za kterých mohou být okrajové módy pozorovány. To zahrnuje analýzu vlivu různých zakončení konečného vlnovodu a různých poměrů ploch průřezů jeho jednotlivých částí. Práce porovnává výhody a nevýhody TMM a SSH modelu s cílem určit, která z metod poskytuje více vypovídající výsledky o vlastnostech vlnovodu. Vybrané výpočty a symbolická odvození se provádějí pomocí softwaru Maple a jsou přiloženy k této práci.

Klíčová slova:
Su-Schrieffer-Heegerův model; metoda matice přechodu; lokálně periodické struktury; objemové módy; okrajové módy; zakázaný pás; Bloch-Floquetův teorém

Název česky:
Rezonanční a přenosové vlastnosti periodického binárního akustického vlnovodu

Contents

Chapter 1

Introduction

Sonic crystals and phononic crystals are specifically designed to manipulate acoustic or elastic waves. They use periodic arrangements to create frequency band gaps that block certain frequencies. Their finite-length versions, which are locally periodic structures, function as topological metamaterials. In these materials, edge conditions alter dispersion, making them effective as topological insulators or wave filters. The bulk-edge correspondence links the bulk characteristics (bulk bound states, bulk modes) of these materials to the existence of edge bound states (edge modes) at the boundaries of the structure [1, 2]. This relationship can be predicted through the winding number [3] or the Zak phase [4, 5]. The edge modes, which are localized at the boundaries within the band gap, are robust against disorder due to topological protection [6], and remain unaffected by defects or irregularities. Notably, the shift from trivial phases, which do not have protected edge modes, to nontrivial phases, which are marked by the presence of such states, is contingent on altering coupling (hopping) coefficients [7]. This highlights the intricate relationship between topology and material design in controlling wave transmission.

In the study of transmission and scattering in locally periodic structures, the transmission matrix method (TMM) is often used [8]. The Su-Schrieffer-Heeger (SSH) 1D model, originally developed for conjugated polymers such as polyacetylene [6], has found wide applications in various fields, including contrast acoustic and elastic media (e.g., [9, 10, 11, 12]), optics (e.g., [13]), vibrational mechanics (e.g., [3, 14]), and electrical circuit systems (e.g., [15]), due to its simple but powerful approach to emulate tight-binding systems via coupling coefficients. The versatility of this model and its predictive capability make it an effective tool for the investigation of one-dimensional topological systems. Locally periodic structures for acoustic fields have been implemented by methods such as binary waveguides with different cross sections [11], alternating resonators [1, 2, 10], periodic deployment of identical scatterers [16], or the construction of duct segments with equally spaced electroacoustic resonators tuned by active feedback [17].

The SSH model provides a solid foundation for exploring key concepts of locally periodic structures such as the Bloch theorem, chiral symmetries and topological invariants. While the TMM and SSH-based methods can benefit from the insights of the Bloch-Floquet theory [18], the TMM stands out primarily for its versatility, while lagging behind in the study of topological phase transitions. The SSH model is easily applicable to binary structures, but the Bloch-Floquet theory is not as effective for binary acoustic waveguides with the same characteristic impedance. Selecting the most suitable method or a combination thereof is crucial for the thorough analysis of specific locally periodic structures.

This thesis is structured as follows. Chapter 2 focuses on the application of the Transfer Matrix Method (TMM) to locally periodic binary acoustic structures. This analysis enables us to establish the relationships necessary for applying the discrete Su-Schrieffer-Heeger (SSH) model to both infinite and finite structures in Chapter 3. These methodologies allow us to concentrate on analysing the frequency and transmission properties of the structures under consideration

and to investigate how they change under different boundary conditions. In Chapter 4, we perform numerical calculations and comparative analyses, and Chapter 5 provides a review and assessment of the effectiveness and suitability of each method. The conclusion is presented in Chapter 6. In addition, Appendix A contains a list of scripts in Maple software that were used in this thesis for selected symbolic and numerical results.

Chapter 2

Transfer Matrix Method (TMM)

2.1 Periodic Binary Acoustic Waveguide

Consider a binary acoustic waveguide filled with air (assumed to be an ideal gas), where elements with cross-sectional areas S_A and S_B alternate periodically as displayed in Fig. 2.1.

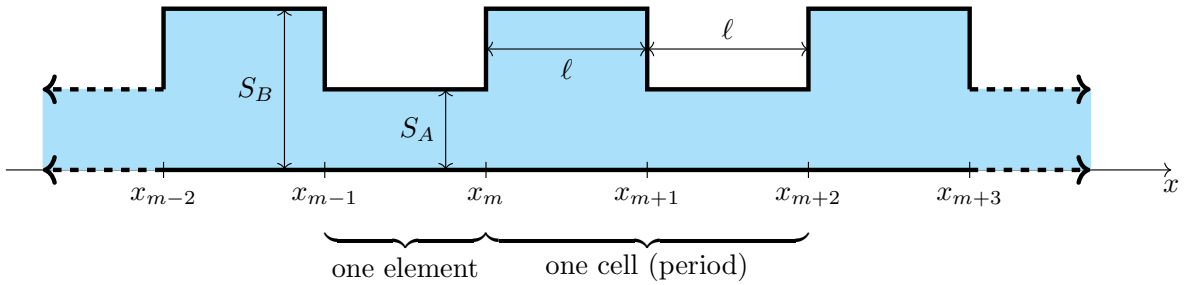

Fig. 2.1: The considered periodic binary acoustic waveguide with cross-sectional areas S_A and S_B and element length ℓ.

Considering a waveguide with a rectangular cross-section, its cutoff frequency is

$$f_\mathrm{c} = \frac{c_0}{2h}, \tag{2.1}$$

where c_0 is the speed of acoustic wave propagation in the fluid filling the waveguide, and h is the longer side of the rectangle [19].
For a waveguide with a circular cross-section of radius r, the cutoff frequency is determined as follows [19]:

$$f_\mathrm{c} = \frac{1.84 c_0}{2\pi r}. \tag{2.2}$$

For frequencies below the cutoff frequency corresponding to the given waveguide element, this element supports plane harmonic acoustic waves along the x-axis which are the solution to the following one-dimensional wave equation:

$$\frac{\partial^2 p(x,t)}{\partial x^2} = \frac{1}{c_0^2}\frac{\partial^2 p(x,t)}{\partial t^2}, \tag{2.3}$$

where $p(x,t)$ is the acoustic pressure and t is time. Considering plane harmonic waves, we can write:

$$p'(x,t) = \mathrm{Re}[P(x)e^{\mathrm{j}\psi}e^{-\mathrm{j}\omega t}] = \mathrm{Re}[\tilde{P}(x)e^{-\mathrm{j}\omega t}], \tag{2.4}$$

and the wave equation is then transformed to the following one-dimensional Helmholtz equation:

$$\frac{\mathrm{d}^2 P(x)}{\mathrm{d}x^2} + k^2 P(x) = 0, \tag{2.5}$$

where $P(x)$ represents the real amplitude of the acoustic pressure, $\omega = 2\pi f$ is the angular frequency, f is the frequency and $k = \omega/c_0$ is the wave number.
Between individual elements of the waveguide, the following continuity conditions must be met at locations where there is a step change in the cross-sectional area between the adjacent elements of the waveguide [11]:

$$[P(x_m)] = 0, \tag{2.6}$$

$$\left[S(x_m) \left(\frac{\mathrm{d}P(x)}{\mathrm{d}x} \right)_{x=x_m} \right] = 0, \tag{2.7}$$

where $S(x_m)$ is a binary function of the cross-sectional area and for $[X(x_m)]$, it holds that

$$[X(x_m)] = \lim_{\epsilon \to 0} [X(x_m + \epsilon) - X(x_m - \epsilon)] \equiv X\left(x_m^+\right) - X\left(x_m^-\right). \tag{2.8}$$

In this case, x_m denotes the location of the step change in the cross-sectional area. In the following text, these step changes are referred to as edges.

Since we assume plane acoustic waves, we consider a linearized one-dimensional Euler equation:

$$\rho_0 \frac{\partial u(x,t)}{\partial t} = -\frac{\partial p'(x,t)}{\partial x}, \tag{2.9}$$

where $u(x,t)$ represents the harmonic acoustic velocity and ρ_0 is the rest density of the considered fluid (an ideal gas in our case). For plane harmonic waves, $p'(x,t)$ is given by Eq. (2.4) and we can write that

$$u(x,t) = \mathrm{Re}\left[U(x) e^{\mathrm{j}\psi} e^{-\mathrm{j}\omega t} \right] = \mathrm{Re}\left[\tilde{U}(x) e^{-\mathrm{j}\omega t} \right], \tag{2.10}$$

where $U(x)$ is the real amplitude of the acoustic velocity.

We introduce positive coupling coefficients v and w as follows:

$$v = \frac{S_A}{S_A + S_B}, \quad w = \frac{S_B}{S_A + S_B} \quad \Longrightarrow \quad v + w = 1. \tag{2.11}$$

The plane harmonic acoustic wave approximation is valid for cross-sectional scales that are considerably smaller than the wavelength of the acoustic wave. The values of S_A and S_B are chosen so that the propagating waves can be considered as plane harmonic waves and thus satisfy Eq. (2.4).

2.2 Transfer Matrix

To describe the acoustic field in a locally periodic structure, the analysis begins with wave propagation through a basic cell, the fundamental component of these structures. Different boundary conditions are applied to study the acoustic field in various types of binary acoustic waveguides, with a focus on examining their transmission properties.
Within this thesis, boundary conditions are categorized into Dirichlet conditions (in our case, Dirichlet condition means that at the corresponding boundary point, $P = 0$) and Neumann conditions (at the corresponding point, $\mathrm{d}P(x)/\mathrm{d}x = 0$).

2.2.1 Single-cell Structure

The basic unit of the periodic structure is a cell depicted in Fig. 2.2. This cell is composed of two elements with respective cross-sectional areas S_A and S_B, and each element has length ℓ.
The acoustic field within each region is characterized by the solutions to the Helmholtz equation, as shown in Eq. (2.5):

Region I
For Region I, the solution $P^{(\mathrm{I})}(x)$ can be expressed as stated below.

$$P^{(\mathrm{I})}(x) = P_+^{(\mathrm{I})}(x) + P_-^{(\mathrm{I})}(x) = Ae^{\mathrm{j}kx} + Be^{-\mathrm{j}kx}, \quad x \le x_0. \tag{2.12}$$

Constants A and B are complex amplitudes determined by boundary conditions. The individual terms of the solution can be conveniently rewritten into the following column vector form:

$$\Psi^{(\mathrm{I})}(x) = \begin{pmatrix} P_+^{(\mathrm{I})}(x) \\ P_-^{(\mathrm{I})}(x) \end{pmatrix} = \begin{pmatrix} Ae^{\mathrm{j}kx} \\ Be^{-\mathrm{j}kx} \end{pmatrix}. \tag{2.13}$$

Analogously, we can write solutions for Regions II and III:

Region II

$$P^{(\mathrm{II})}(x) = P_+^{(\mathrm{II})}(x) + P_-^{(\mathrm{II})}(x) = Fe^{\mathrm{j}kx} + Ge^{-\mathrm{j}kx}, \quad x_0 \le x \le x_0 + \ell, \tag{2.14}$$

$$\Psi^{(\mathrm{II})}(x) = \begin{pmatrix} P_+^{(\mathrm{II})}(x) \\ P_-^{(\mathrm{II})}(x) \end{pmatrix} = \begin{pmatrix} Fe^{\mathrm{j}kx} \\ Ge^{-\mathrm{j}kx} \end{pmatrix}. \tag{2.15}$$

Region III

$$P^{(\mathrm{III})}(x) = P_+^{(\mathrm{III})}(x) + P_-^{(\mathrm{III})}(x) = Ce^{\mathrm{j}kx} + De^{-\mathrm{j}kx}, \quad x_0 + \ell \le x \le x_0 + 2\ell, \tag{2.16}$$

$$\Psi^{(\mathrm{III})}(x) = \begin{pmatrix} P_+^{(\mathrm{III})}(x) \\ P_-^{(\mathrm{III})}(x) \end{pmatrix} = \begin{pmatrix} Ce^{\mathrm{j}kx} \\ De^{-\mathrm{j}kx} \end{pmatrix}. \tag{2.17}$$

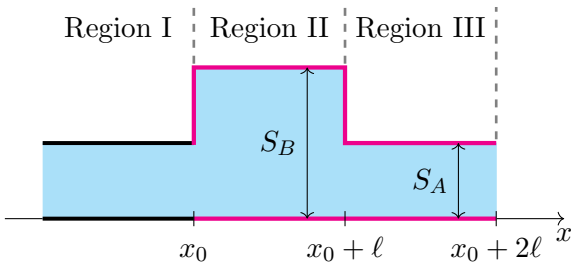

Fig. 2.2: A diagram of the considered cell with designated Regions I, II and III. The cell boundaries are marked in red.

For the considered cell of the periodic structure, we can now derive its transfer matrix. First, we focus on Region II, for which the following relationship between column vectors can be written:

$$\begin{pmatrix} P_+^{(\mathrm{II})}(x_0+\ell) \\ P_-^{(\mathrm{II})}(x_0+\ell) \end{pmatrix} = \begin{pmatrix} \frac{P_+^{(\mathrm{II})}(x_0+\ell)}{P_+^{(\mathrm{II})}(x_0)} & 0 \\ 0 & \frac{P_-^{(\mathrm{II})}(x_0+\ell)}{P_-^{(\mathrm{II})}(x_0)} \end{pmatrix} \begin{pmatrix} P_+^{(\mathrm{II})}(x_0) \\ P_-^{(\mathrm{II})}(x_0) \end{pmatrix} = \mathbf{M}^{(\rightarrow)} \begin{pmatrix} P_+^{(\mathrm{II})}(x_0) \\ P_-^{(\mathrm{II})}(x_0) \end{pmatrix}, \tag{2.18}$$

that is

$$\Psi^{(\mathrm{II})}(x_0+\ell) = \begin{pmatrix} e^{\mathrm{j}k\ell} & 0 \\ 0 & e^{-\mathrm{j}k\ell} \end{pmatrix} \Psi^{(\mathrm{II})}(x_0) = \mathbf{M}^{(\rightarrow)} \Psi^{(\mathrm{II})}(x_0). \tag{2.19}$$

Employing Eqs. (2.6) and (2.7), the following continuity conditions must be met between the solutions for Region I (with the cross-section S_A) and for Region II (with the cross-section S_B):

$$P^{(\mathrm{I})}(x_0) = P^{(\mathrm{II})}(x_0), \tag{2.20}$$

$$S_A \left(\frac{\mathrm{d}P^{(\mathrm{I})}(x)}{\mathrm{d}x} \right)_{x_{0-}} = S_B \left(\frac{\mathrm{d}P^{(\mathrm{II})}(x)}{\mathrm{d}x} \right)_{x_{0+}} \xrightarrow{\times \frac{1}{S_A+S_B}} v \left(\frac{\mathrm{d}P^{(\mathrm{I})}(x)}{\mathrm{d}x} \right)_{x_{0-}} = w \left(\frac{\mathrm{d}P^{(\mathrm{II})}(x)}{\mathrm{d}x} \right)_{x_{0+}}, \tag{2.21}$$

where v and w denote the coupling coefficients introduced in Eq. (2.11). If we expand these continuity conditions, we obtain the following system of two equations:

$$Ae^{\mathrm{j}kx_0} + Be^{-\mathrm{j}kx_0} = Fe^{\mathrm{j}kx_0} + Ge^{-\mathrm{j}kx_0}, \tag{2.22}$$

$$\mathrm{j}kv \left(Ae^{\mathrm{j}kx_0} - Be^{-\mathrm{j}kx_0} \right) = \mathrm{j}kw \left(Fe^{\mathrm{j}kx_0} - Ge^{-\mathrm{j}kx_0} \right), \tag{2.23}$$

or equivalently:

$$P_+^{(\mathrm{I})}(x_0) + P_-^{(\mathrm{I})}(x_0) = P_+^{(\mathrm{II})}(x_0) + P_-^{(\mathrm{II})}(x_0), \tag{2.24}$$

$$v \left[P_+^{(\mathrm{I})}(x_0) - P_-^{(\mathrm{I})}(x_0) \right] = w \left[P_+^{(\mathrm{II})}(x_0) - P_-^{(\mathrm{II})}(x_0) \right]. \tag{2.25}$$

Eqs. (2.24) and (2.25) can be rewritten in matrix form as follows:

$$\begin{pmatrix} 1 & 1 \\ v & -v \end{pmatrix} \begin{pmatrix} P_+^{(\mathrm{I})}(x_0) \\ P_-^{(\mathrm{I})}(x_0) \end{pmatrix} = \begin{pmatrix} 1 & 1 \\ w & -w \end{pmatrix} \begin{pmatrix} P_+^{(\mathrm{II})}(x_0) \\ P_-^{(\mathrm{II})}(x_0) \end{pmatrix}. \tag{2.26}$$

From this, we obtain:

$$\begin{pmatrix} P_+^{(\mathrm{II})}(x_0) \\ P_-^{(\mathrm{II})}(x_0) \end{pmatrix} = \begin{pmatrix} 1 & 1 \\ w & -w \end{pmatrix}^{-1} \begin{pmatrix} 1 & 1 \\ v & -v \end{pmatrix} \begin{pmatrix} P_+^{(\mathrm{I})}(x_0) \\ P_-^{(\mathrm{I})}(x_0) \end{pmatrix} = \frac{1}{2w} \begin{pmatrix} w+v & w-v \\ w-v & w+v \end{pmatrix} \begin{pmatrix} P_+^{(\mathrm{I})}(x_0) \\ P_-^{(\mathrm{I})}(x_0) \end{pmatrix} = \mathbf{M}^{(\uparrow)} \begin{pmatrix} P_+^{(\mathrm{I})}(x_0) \\ P_-^{(\mathrm{I})}(x_0) \end{pmatrix}. \quad (2.27)$$

Similarly, between the solutions for Region II with the cross-section S_B and for Region III with the cross-section S_A, the following continuity conditions must be met:

$$P^{(\mathrm{II})}(x_0+\ell) = P^{(\mathrm{III})}(x_0+\ell), \quad (2.28)$$

$$w \left(\frac{\mathrm{d}P^{(\mathrm{II})}(x)}{\mathrm{d}x} \right)_{(x_0+\ell)_-} = v \left(\frac{\mathrm{d}P^{(\mathrm{III})}(x)}{\mathrm{d}x} \right)_{(x_0+\ell)_+}. \quad (2.29)$$

We now expand these continuity conditions as follows:

$$P_+^{(\mathrm{II})}(x_0+\ell) + P_-^{(\mathrm{II})}(x_0+\ell) = P_+^{(\mathrm{III})}(x_0+\ell) + P_-^{(\mathrm{III})}(x_0+\ell), \quad (2.30)$$

$$w \left[P_+^{(\mathrm{II})}(x_0+\ell) - P_-^{(\mathrm{II})}(x_0+\ell) \right] = v \left[P_+^{(\mathrm{III})}(x_0+\ell) - P_-^{(\mathrm{III})}(x_0+\ell) \right]. \quad (2.31)$$

Again, we rewrite the system of Eqs. (2.30) and (2.31) in matrix form:

$$\begin{pmatrix} 1 & 1 \\ w & -w \end{pmatrix} \begin{pmatrix} P_+^{(\mathrm{II})}(x_0+\ell) \\ P_-^{(\mathrm{II})}(x_0+\ell) \end{pmatrix} = \begin{pmatrix} 1 & 1 \\ v & -v \end{pmatrix} \begin{pmatrix} P_+^{(\mathrm{III})}(x_0+\ell) \\ P_-^{(\mathrm{III})}(x_0+\ell) \end{pmatrix}. \quad (2.32)$$

From this, we obtain:

$$\begin{pmatrix} P_+^{(\mathrm{III})}(x_0+\ell) \\ P_-^{(\mathrm{III})}(x_0+\ell) \end{pmatrix} = \begin{pmatrix} 1 & 1 \\ v & -v \end{pmatrix}^{-1} \begin{pmatrix} 1 & 1 \\ w & -w \end{pmatrix} \begin{pmatrix} P_+^{(\mathrm{II})}(x_0+\ell) \\ P_-^{(\mathrm{II})}(x_0+\ell) \end{pmatrix} = \frac{1}{2v} \begin{pmatrix} w+v & v-w \\ v-w & w+v \end{pmatrix} \begin{pmatrix} P_+^{(\mathrm{II})}(x_0+\ell) \\ P_-^{(\mathrm{II})}(x_0+\ell) \end{pmatrix} = \mathbf{M}^{(\downarrow)} \begin{pmatrix} P_+^{(\mathrm{II})}(x_0+\ell) \\ P_-^{(\mathrm{II})}(x_0+\ell) \end{pmatrix}. \quad (2.33)$$

Based on Eqs. (2.18), (2.27), and (2.33), we can write:

$$\Psi^{(\mathrm{III})}(x_0+\ell) = \mathbf{M}^{(\downarrow)}\mathbf{M}^{(\rightarrow)}\mathbf{M}^{(\uparrow)}\Psi^{(\mathrm{I})}(x_0) = \mathbf{M}^{(\mathrm{II})}\Psi^{(\mathrm{I})}(x_0), \quad (2.34)$$

where $\mathbf{M}^{(\mathrm{II})}$ is the transfer matrix of the element with the cross-section S_B, which can be expressed as follows:

$$\mathbf{M}^{(\mathrm{II})} = \mathbf{M}^{(\downarrow)}\mathbf{M}^{(\rightarrow)}\mathbf{M}^{(\uparrow)} = \frac{1}{2vw} \begin{pmatrix} 2vw\cos(k\ell) + \mathrm{j}\left(v^2+w^2\right)\sin(k\ell) & -\mathrm{j}\left(v^2-w^2\right)\sin(k\ell) \\ \mathrm{j}\left(v^2-w^2\right)\sin(k\ell) & 2vw\cos(k\ell) - \mathrm{j}\left(v^2+w^2\right)\sin(k\ell) \end{pmatrix}. \quad (2.35)$$

Similarly, for Region III, the relationship between column vectors can be written as:

$$\begin{pmatrix} P_+^{(\mathrm{III})}(x_0+2\ell) \\ P_-^{(\mathrm{III})}(x_0+2\ell) \end{pmatrix} = \begin{pmatrix} \frac{P_+^{(\mathrm{III})}(x_0+2\ell)}{P_+^{(\mathrm{III})}(x_0+\ell)} & 0 \\ 0 & \frac{P_-^{(\mathrm{III})}(x_0+2\ell)}{P_-^{(\mathrm{III})}(x_0+\ell)} \end{pmatrix} \begin{pmatrix} P_+^{(\mathrm{III})}(x_0+\ell) \\ P_-^{(\mathrm{III})}(x_0+\ell) \end{pmatrix} = \mathbf{M}^{(\rightarrow)} \begin{pmatrix} P_+^{(\mathrm{III})}(x_0+\ell) \\ P_-^{(\mathrm{III})}(x_0+\ell) \end{pmatrix}, \tag{2.36}$$

that is

$$\Psi^{(\mathrm{III})}(x_0+2\ell) = \begin{pmatrix} e^{\mathrm{j}k\ell} & 0 \\ 0 & e^{-\mathrm{j}k\ell} \end{pmatrix} \Psi^{(\mathrm{III})}(x_0+\ell) = \mathbf{M}^{(\rightarrow)} \Psi^{(\mathrm{III})}(x_0+\ell). \tag{2.37}$$

Comparing Eqs. (2.18) and (2.36), we see that the transfer matrix $\mathbf{M}^{(\rightarrow)}$ takes the same form in both cases as we consider elements of the structure where there is no edge. However, this is only true if the individual edges in the considered structure are equidistant, i.e., if the length ℓ is the distance between all the adjacent edges.
Using Eqs. (2.34) and (2.37), it can be stated that

$$\Psi^{(\mathrm{III})}(x_0+2\ell) = \mathbf{M}^{(\rightarrow)}\mathbf{M}^{(\mathrm{II})}\Psi^{(\mathrm{I})}(x_0) = \mathbf{M}^{(\rightarrow)}\mathbf{M}^{(\downarrow)}\mathbf{M}^{(\rightarrow)}\mathbf{M}^{(\uparrow)}\Psi^{(\mathrm{I})}(x_0) = \mathbf{M}\Psi^{(\mathrm{I})}(x_0), \tag{2.38}$$

where $\mathbf{M}$ is the desired transfer matrix of the entire cell and it is given as follows:

$$\mathbf{M} = \frac{1}{2vw} \begin{pmatrix} e^{\mathrm{j}k\ell}\left[2vw\cos(k\ell) + \mathrm{j}\left(v^2+w^2\right)\sin(k\ell)\right] & -e^{\mathrm{j}k\ell}\mathrm{j}\left(v^2-w^2\right)\sin(k\ell) \\ e^{-\mathrm{j}k\ell}\mathrm{j}\left(v^2-w^2\right)\sin(k\ell) & e^{-\mathrm{j}k\ell}\left[2vw\cos(k\ell) - \mathrm{j}\left(v^2+w^2\right)\sin(k\ell)\right] \end{pmatrix}. \tag{2.39}$$

Employing Eq. (2.39), we introduce the following notation for components of the transfer matrix:

$$\mathbf{M} = \begin{pmatrix} M_{11} & M_{12} \\ M_{21} & M_{22} \end{pmatrix} = \begin{pmatrix} M_{11} & M_{12} \\ M_{12}^* & M_{11}^* \end{pmatrix} = \begin{pmatrix} a & b \\ b^* & a^* \end{pmatrix}. \tag{2.40}$$

Additionaly, it holds that $\det(\mathbf{M}) = 1$ and thus $\mathbf{M}$ is a unimodular matrix.

2.2.2 Multi-cell Structure

The eigenvalues ε of the transfer matrix $\mathbf{M}$ represent solutions of the following quadratic equation:

$$\det(\mathbf{M} - \varepsilon\mathbf{I}) = \varepsilon^2 - \underbrace{(a+a^*)}_{\mathrm{Tr}\,\mathbf{M}}\varepsilon + \underbrace{aa^* - bb^*}_{\det(\mathbf{M})=1} = 0. \tag{2.41}$$

By substituting $\varepsilon = e^{\mathrm{j}q}$, we obtain:

$$e^{2\mathrm{j}q} - e^{\mathrm{j}q}\,\mathrm{Tr}\,\mathbf{M} + 1 = 0. \tag{2.42}$$

When multiplied by $e^{-\mathrm{j}q}$, the result is as follows:

$$e^{\mathrm{j}q} - \mathrm{Tr}\,\mathbf{M} + e^{-\mathrm{j}q} = 0. \tag{2.43}$$

After adjustments, we can write that

$$\cos q = \frac{1}{2}\operatorname{Tr}\mathbf{M} = \xi. \tag{2.44}$$

In the Bloch theory concerning periodic 1D systems, ξ is called the Bloch phase and q represents the dimensionless Bloch wave number [20]. More details are provided in Section 3.2.
We can determine the solutions of Eq. (2.41) (i.e., the eigenvalues $\varepsilon_{\pm}$) as:

$$\varepsilon_{\pm} = \frac{\operatorname{Tr}\mathbf{M} \pm \sqrt{(\operatorname{Tr}\mathbf{M})^2 - 4}}{2} = \cos(q) \pm \mathrm{j}\sin(q) = e^{\pm \mathrm{j}q}. \tag{2.45}$$

If we consider an infinite periodic structure comprised of identical cells (each with the transfer matrix $\mathbf{M}$), then ξ is given by the following relation:

$$\xi = \frac{1}{2}\operatorname{Tr}\mathbf{M} = \frac{1}{2}\left(a + a^*\right) = \frac{(v+w)^2\cos(2k\ell) - (v-w)^2}{4vw} = \frac{\cos(2k\ell) - (v-w)^2}{4vw}. \tag{2.46}$$

Using the identity

$$\cos(2k\ell) = 2\cos^2(k\ell) - 1,$$

we can modify this result for the Bloch phase in the form:

$$\xi = \frac{(v+w)^2\left[2\cos^2(k\ell) - 1\right] - (v-w)^2}{4vw} = \frac{2(v+w)^2\cos^2(k\ell) - (v+w)^2 - (v-w)^2}{4vw} = \frac{(v+w)^2\cos^2(k\ell) - (v^2+w^2)}{2vw}. \tag{2.47}$$

From this, we obtain:

$$(v+w)^2\cos^2(k\ell) = v^2 + w^2 + 2vw\xi. \tag{2.48}$$

Considering that $v+w=1$ and employing the notation from Eq. (2.44), the following relationship can be written:

$$\boxed{\cos(k\ell) = \pm\sqrt{v^2 + w^2 + 2vw\cos(q)}.} \tag{2.49}$$

We consider a locally periodic structure consisting of N cells (see Fig. 2.3), for which, without loss of generality, we choose $x_0 = 0$. Since the length of one cell is equal to 2ℓ, we can write that

$$\Psi(x = 2N\ell) = \mathbf{M}^N\Psi(x = 0), \tag{2.50}$$

where

$$\Psi(x = 2N\ell) = \begin{pmatrix} P_+(x = 2N\ell) \\ P_-(x = 2N\ell) \end{pmatrix} = \begin{pmatrix} A_N e^{\mathrm{j}2kN\ell} \\ B_N e^{\mathrm{j}2kN\ell} \end{pmatrix}, \tag{2.51}$$

and

$$\Psi(x = 0) = \begin{pmatrix} P_+(x = 0) \\ P_-(x = 0) \end{pmatrix} = \begin{pmatrix} A_0 \\ B_0 \end{pmatrix}. \tag{2.52}$$

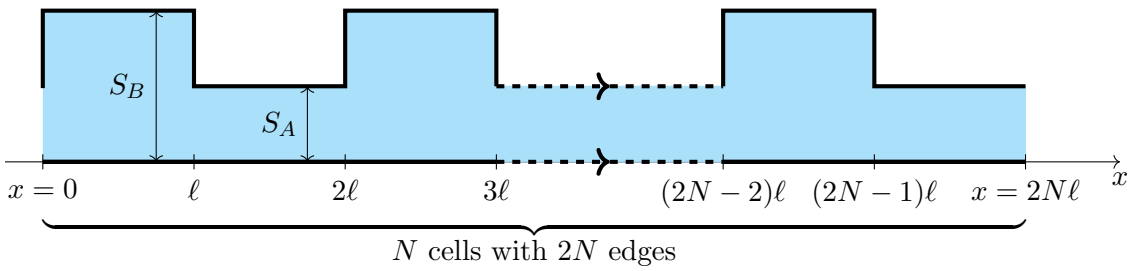

Fig. 2.3: A diagram of the finite locally periodic structure composed of multiple cells.

The Nth power of the matrix $\mathbf{M}$ can be calculated using the Cayley-Hamilton theorem. This theorem states that every matrix satisfies its own characteristic equation [21]. For the Nth power of any unimodular matrix $\mathbf{M}$, we can write the following closed-form expression [20]:

$$\mathbf{M}^N = \mathbf{M}U_{N-1}(\xi) - \mathbf{I}U_{N-2}(\xi), \tag{2.53}$$

where $U_N(\xi)$ is the Chebyshev polynomial of the second kind, of degree N, evaluated at ξ, and $\mathbf{I}$ is the identity matrix. Employing the notation from Eq. (2.40), we can write:

$$\mathbf{M}^N = \begin{pmatrix} a & b \\ b^* & a^* \end{pmatrix}^N = \begin{pmatrix} a_N & b_N \\ b_N^* & a_N^* \end{pmatrix} = \begin{pmatrix} aU_{N-1}(\xi) - U_{N-2}(\xi) & bU_{N-1}(\xi) \\ b^*U_{N-1}(\xi) & a^*U_{N-1}(\xi) - U_{N-2}(\xi) \end{pmatrix}. \tag{2.54}$$

The Chebyshev polynomial $U_N(\xi)$ can be expressed using the sine function as follows [22]:

$$U_N(\xi) = \frac{\sin\left[(N+1)q\right]}{\sin(q)}, \tag{2.55}$$

where $q = \arccos(\xi)$.
Using Eq. (2.55), we can express $\mathbf{M}^N$ as:

$$\boxed{\mathbf{M}^N = \frac{1}{\sin(q)} \begin{pmatrix} a\sin(Nq) - \sin[(N-1)q] & b\sin(Nq) \\ b^*\sin(Nq) & a^*\sin(Nq) - \sin[(N-1)q] \end{pmatrix}.} \tag{2.56}$$

From the Bloch theory, it follows that waves with frequencies for which the relation $|\xi| > 1$ holds cannot propagate through a periodic structure. The frequency interval with this property represents the so-called band gap (forbidden band).
By differentiating the Bloch phase (2.46) with respect to the wave number k, we find that it attains extreme values for $2k\ell = n\pi$, where n is an integer. From the second derivative of the Bloch phase, we determine that it reaches a local maximum for even n and a local minimum for odd n. Substituting the stationary points corresponding to the local maximum into Eq. (2.46), we find that for these, the Bloch phase attains a value of one, hence only local minima are found in the band gaps.
The Bloch phase ξ for a particular waveguide is shown in Fig. 2.4.

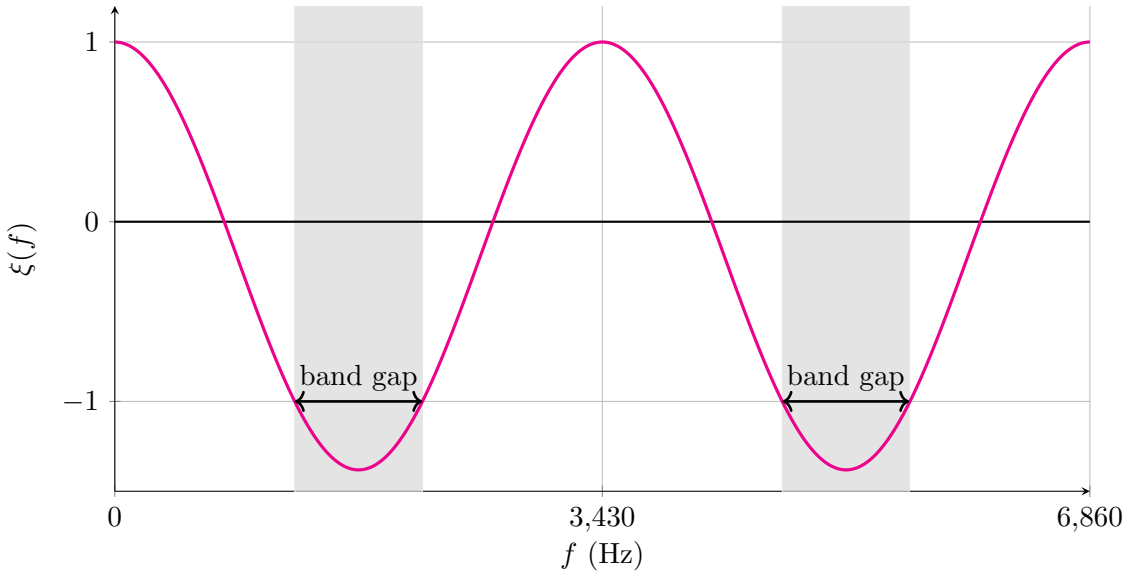

Fig. 2.4: The Bloch phase ξ of a particular waveguide. Values of chosen parameters: $c_0 = 343$ ms^{-1}, $\ell = 0.05$ m, $f \in [0; 6{,}860]$ Hz, and the coupling coefficient $v = 0.3$. Frequencies on which $\xi = -1$ delimit the band gaps.

In the case of an open finite structure, we consider that the acoustic field does not extend beyond the boundaries of the waveguide, meaning it is not radiated beyond the open edges into the surroundings. Assuming finite periodic structure as a resonator with open ends, then it must hold that the pressure is zero at both its ends, i.e., $P(x = 0) = 0$ and $P(x = 2N\ell) = 0$. This means that $P_-(x = 0) = -P_+(x = 0)$ and $P_-(x = 2N\ell) = -P_+(x = 2N\ell)$. Including these boundary conditions in Eq. (2.50), we obtain the following equation:

$$\begin{aligned} P_+(x = 2N\ell) \begin{pmatrix} 1 \\ -1 \end{pmatrix} = P_+(x = 0)\, \mathbf{M}^N \begin{pmatrix} 1 \\ -1 \end{pmatrix} = \\ \frac{P_+(x = 0)}{\sin(q)} \begin{pmatrix} a\sin(Nq) - \sin[(N-1)q] & b\sin(Nq) \\ b^*\sin(Nq) & a^*\sin(Nq) - \sin[(N-1)q] \end{pmatrix} \begin{pmatrix} 1 \\ -1 \end{pmatrix} = \\ \frac{P_+(x = 0)}{\sin(q)} \begin{pmatrix} (a-b)\sin(Nq) - \sin[(N-1)q] \\ (b^*-a^*)\sin(Nq) + \sin[(N-1)q] \end{pmatrix}. \end{aligned} \tag{2.57}$$

Now, we multiply this equation from the left by the row vector $\begin{pmatrix} 1 & 1 \end{pmatrix}$, thereby obtaining:

$$P_+(x = 2N\ell) \begin{pmatrix} 1 & 1 \end{pmatrix} \begin{pmatrix} 1 \\ -1 \end{pmatrix} = \frac{P_+(x = 0)}{\sin(q)} \begin{pmatrix} 1 & 1 \end{pmatrix} \begin{pmatrix} (a-b)\sin(Nq) - \sin[(N-1)q] \\ (b^*-a^*)\sin(Nq) + \sin[(N-1)q] \end{pmatrix}. \tag{2.58}$$

Since it holds that

$$\begin{pmatrix} 1 & 1 \end{pmatrix} \begin{pmatrix} 1 \\ -1 \end{pmatrix} = (0), \tag{2.59}$$

then after rearranging Eq. (2.58), we obtain:

$$0 = (a - a^* + b^* - b)\frac{\sin(Nq)}{\sin(q)}. \tag{2.60}$$

This equation can only be satisfied for certain frequencies, known as resonance frequencies (eigenfrequencies) or eigenmodes. By substituting the matrix components from Eq. (2.40) into Eq. (2.60), after simplifications, we can write:

$$0 = \frac{\mathrm{j}(v+w)\sin(2k\ell)\sin(Nq)}{w\sin(q)} = \frac{\mathrm{j}\sin(2k\ell)\sin(Nq)}{w\sin(q)}. \tag{2.61}$$

We introduce the following notation for the expression in Eq. (2.61):

$$\frac{\sin(2k\ell)\sin(Nq)}{\sin(q)} = \eta(f), \tag{2.62}$$

and we can write that

$$\eta(f) = 0. \tag{2.63}$$

For frequencies that satisfy Eq. (2.63), the boundary conditions for the considered locally periodic structure are satisfied. If we assume the case where $\xi < -1$, then for the dimensionless Bloch wave number, we can write:

$$q = \arccos(\xi) = \pi - \mathrm{j}\ln\left(|\xi| + \sqrt{\xi^2 - 1}\right) \quad \text{for} \quad \xi < -1. \tag{2.64}$$

Since the identity $\sin(\mathrm{j}\alpha) = \mathrm{j}\sinh(\alpha)$ holds, where α is a real number, then for the case $\xi < -1$ (i.e., for the band gap), it is possible to solve Eq. (2.63) as

$$\sin(2k\ell)\sinh\left[N\ln\left(|\xi| + \sqrt{\xi^2 - 1}\right)\right] = 0. \tag{2.65}$$

Given that the above-mentioned function $\sinh\left[N\ln\left(|\xi| + \sqrt{\xi^2 - 1}\right)\right]$ does not pass through zero in the band gap, this equation can only be satisfied for $\sin(2k\ell) = 0$ in the band gap:

$$2k\ell = n\pi \quad \Longrightarrow \quad f = \frac{nc_0}{4\ell}, \quad n = 1, 2, \ldots \quad \text{(considering positive frequencies solely)}. \tag{2.66}$$

Eq. (2.62) must be solved in its full form, not just for a zero numerator, because in the band gap where $\xi < -1$, the dimensionless Bloch wave number q takes complex values, as follows from Eq. (2.64).

If we consider only the first band gap, where $n = 1$, which corresponds to the first local minimum of the Bloch phase, this minimum coincides with the frequency for which Eq. (2.65) is satisfied, thus finding the frequency for the edge mode.
The resonance frequencies for particular waveguides are shown in Fig. 2.5. It can be seen that the closer the value of the coupling coefficient v is to the value of w, the smaller is the width of the band gap. For the extreme case $v = w$, the band gap disappears. Within the band gap, the edge modes are determined by Eq. (2.66).

In the next part of this chapter, we introduce and discuss four specific cases of locally periodic structures (see Fig. 2.6). We focus on the properties of wave propagation given by the boundary conditions for each waveguide.

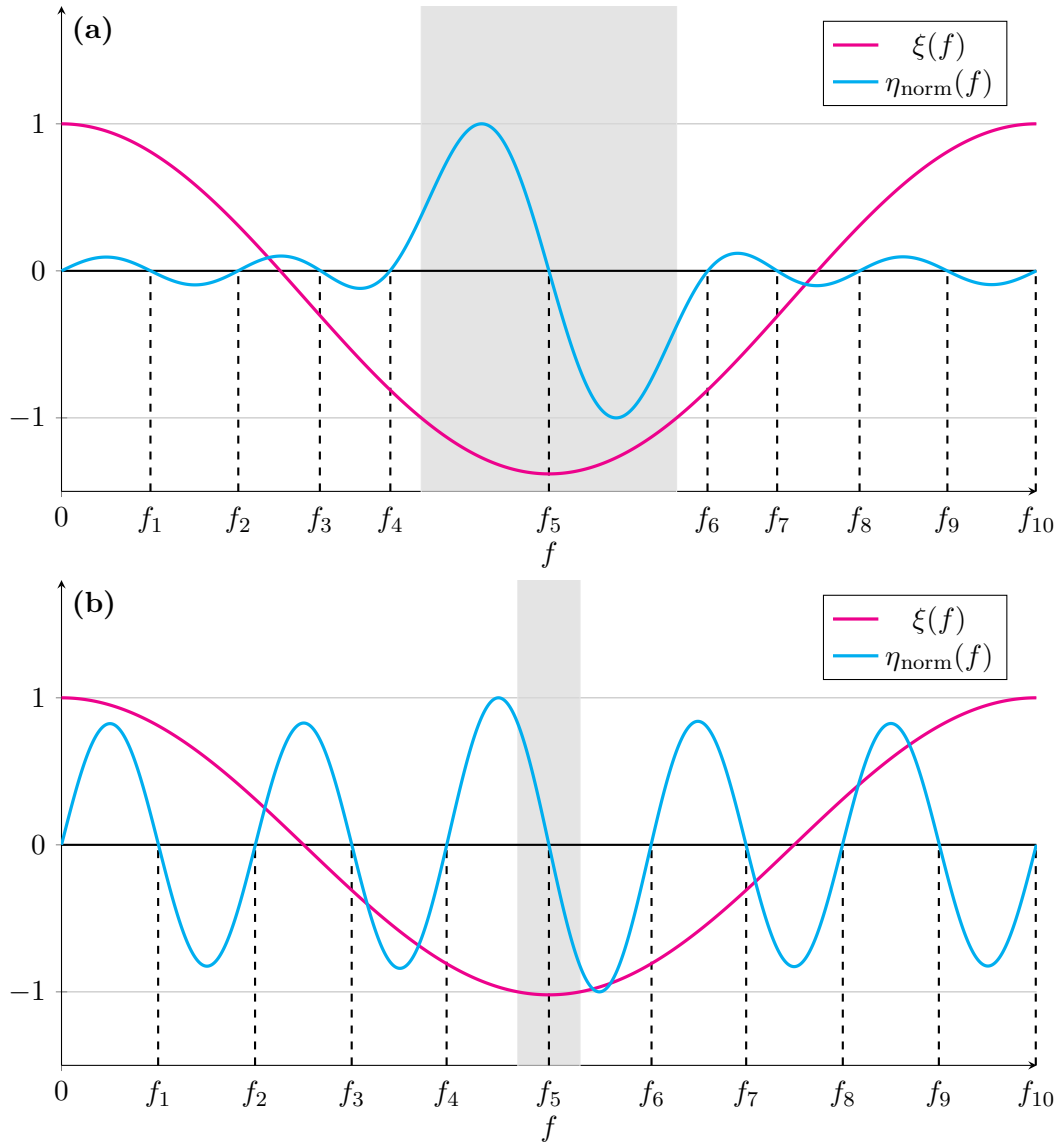

Fig. 2.5: Determination of eigenmodes according to $\xi(f)$ and normalized $\eta(f)$ (denoted as $\eta_{\text{norm}}(f)$). For **(a)** $v = 0.3$, and for **(b)** $v = 0.45$. Values of chosen parameters: $N = 5$, $c_0 = 343$ ms^{-1}, $\ell = 0.05$ m, $f \in [0; f_{10} = 3{,}430]$ Hz. The gray region indicates the frequency range falling within the band gaps.

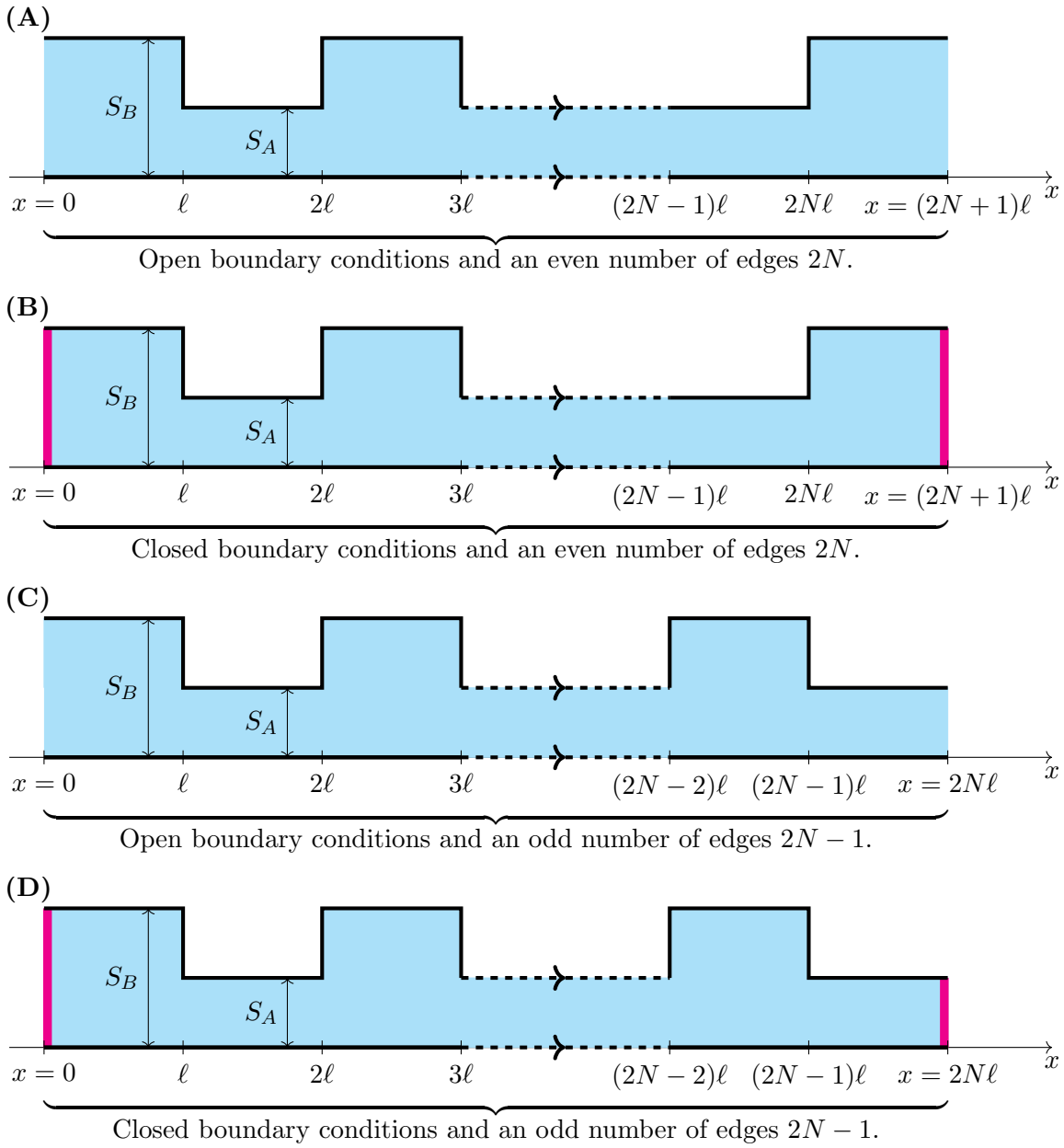

Fig. 2.6: Diagrams of the locally periodic structures composed of multiple cells. The corresponding transfer matrices are $\mathbf{M}_{\mathrm{A}}$ for Cases **(A)** and **(B)** and $\mathbf{M}_{\mathrm{C}}$ for Cases **(C)** and **(D)**. In Cases **(B)** and **(D)**, both ends of the waveguide are closed by a perfectly rigid wall.

(A) Finite locally periodic symmetric structure with open ends

We consider the case where the finite locally periodic structure comprised of $N+1$ cells does not begin with a step change from the cross-section S_A to S_B, see Fig. 2.6**(A)**. In addition, we eliminate the propagation in the element with cross section S_A at the end of this structure, thus obtaining:

$$\mathbf{M}_{\mathrm{A}} = \left(\mathbf{M}^{(\rightarrow)}\mathbf{M}^{(\downarrow)}\right)^{-1} \mathbf{M}^{N+1} \left(\mathbf{M}^{(\uparrow)}\right)^{-1}. \tag{2.67}$$

Considering the Dirichlet boundary conditions for the open ends of the locally periodic structure where $P(x=0)=0$ and $P[x=(2N+1)\ell]=0$, we obtain:

$$(0) = \begin{pmatrix} 1 & 1 \end{pmatrix} \mathbf{M}_{\mathrm{A}} \begin{pmatrix} 1 \\ -1 \end{pmatrix}. \tag{2.68}$$

From this, we get that

$$\frac{2\mathrm{j}\sin(k\ell)\{w\sin(Nq) + v\sin[(N+1)q]\}}{v\sin(q)} = 0. \tag{2.69}$$

In order to find the eigenmodes, this can be rewritten into the form:

$$\frac{\sin(k\ell)\sin(Nq)(w+v\xi)}{v\sin(q)} + \sin(k\ell)\cos(Nq) = \nu(f) = 0, \tag{2.70}$$

where it was used that $\xi = \cos(q)$.

This condition is satisfied for two frequencies falling within the band gap, i.e., there are two edge modes (namely f_5 and f_6), as shown in Fig. 2.7**(A)**.

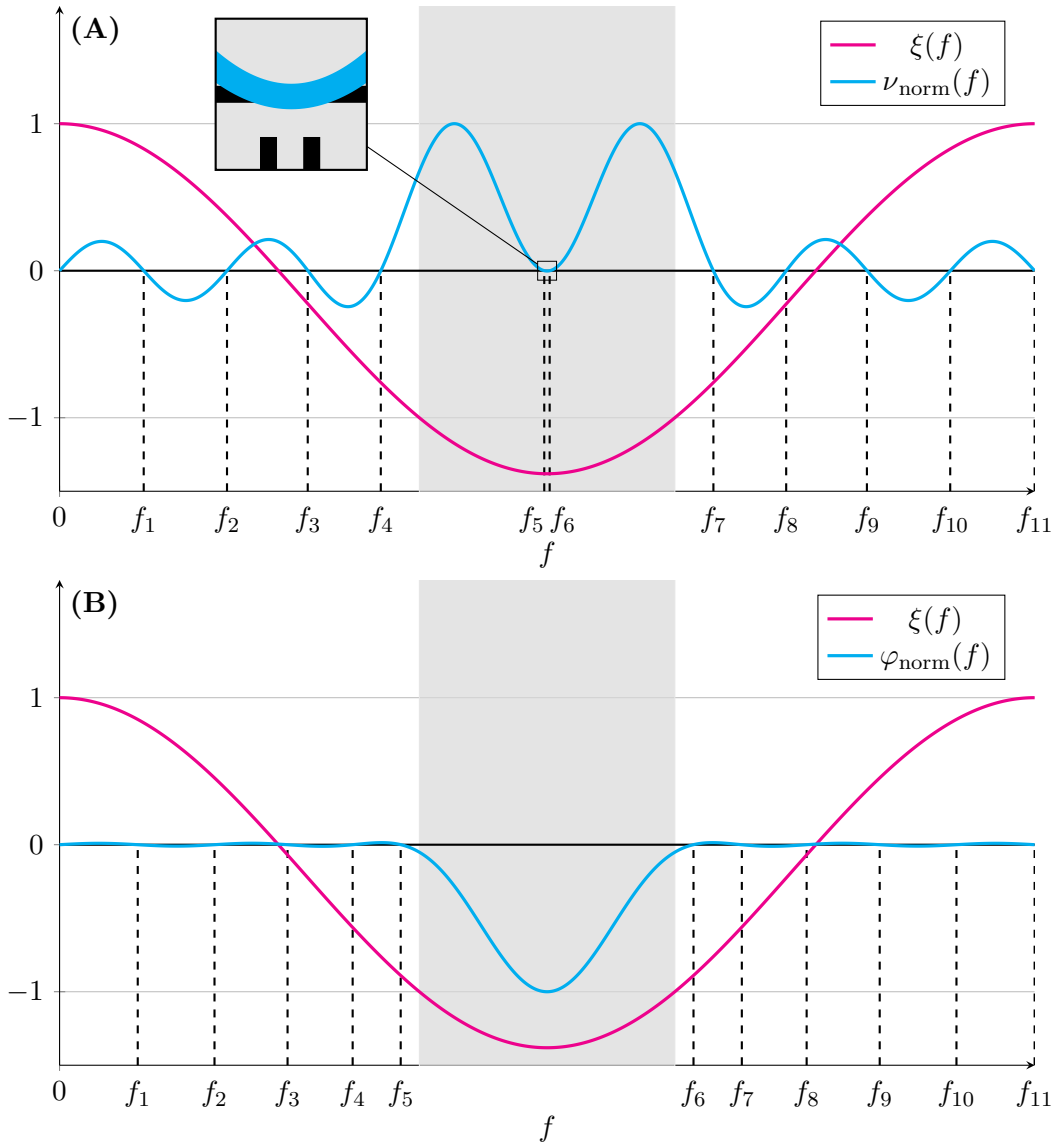

Fig. 2.7: Determination of eigenmodes according to $\xi(f)$ and normalized $\nu(f)$ (denoted as $\nu_{\text{norm}}(f)$) in **(A)**, normalized $\varphi(f)$ (denoted as $\varphi_{\text{norm}}(f)$) in **(B)**. Values of chosen parameters: $N = 5$, $c_0 = 343\,\text{ms}^{-1}$, $\ell = 0.05\,\text{m}$, $f \in [0; f_{11} = 3{,}430]\,\text{Hz}$, and the coupling coefficient $v = 0.3$. The gray region indicates the frequency range falling within the band gap.

(B) Finite locally periodic symmetric structure with closed ends

We now consider the case for the structure corresponding to the transfer matrix $\mathbf{M}_\mathrm{A}$ (formulated in Eq. (2.67)), but its both ends are closed by a perfectly rigid wall, see Fig. 2.6**(B)**. Thus, it differs in the boundary conditions and it must hold that the acoustic velocities at these points are zero (resulting in the derivatives of the acoustic pressure with respect to x being zero at these points). Since it holds that

$$\frac{\mathrm{d}P(x)}{\mathrm{d}x} = \mathrm{j}k\left[P_+(x) - P_-(x)\right], \tag{2.71}$$

then a zero derivative of the acoustic pressure at the points $x = 0$ and $x = (2N+1)\ell$ is ensured by setting

$$P_-(0) = P_+(0), \tag{2.72}$$

$$P_-[(2N+1)\ell] = P_+[(2N+1)\ell], \tag{2.73}$$

at these points, so we can write that

$$P_+[x = (2N+1)\ell]\begin{pmatrix}1\\1\end{pmatrix} = \mathbf{M}_\mathrm{A} P_+(0)\begin{pmatrix}1\\1\end{pmatrix}. \tag{2.74}$$

It also holds that

$$\frac{\mathrm{d}P(x)}{\mathrm{d}x} = \mathrm{j}k\left[P_+(x) - P_-(x)\right] = \mathrm{j}k\begin{pmatrix}1 & -1\end{pmatrix}\begin{pmatrix}P_+(x)\\P_-(x)\end{pmatrix}. \tag{2.75}$$

From this, it is evident that when we multiply Eq. (2.74) from the left by the row vector $\begin{pmatrix}1 & -1\end{pmatrix}$, we get the zero derivative of the pressure (the Neumann boundary condition) at the required points:

$$P_+[x = (2N+1)\ell]\begin{pmatrix}1 & -1\end{pmatrix}\begin{pmatrix}1\\1\end{pmatrix} = P_+(0)\begin{pmatrix}1 & -1\end{pmatrix}\mathbf{M}_\mathrm{A}\begin{pmatrix}1\\1\end{pmatrix}, \tag{2.76}$$

and so we obtain:

$$(0) = \begin{pmatrix}1 & -1\end{pmatrix}\mathbf{M}_\mathrm{A}\begin{pmatrix}1\\1\end{pmatrix}. \tag{2.77}$$

After rearranging, we obtain that

$$\frac{2\mathrm{j}\sin(k\ell)\{v\sin(Nq) + w\sin[(N+1)q]\}}{w\sin(q)} = 0. \tag{2.78}$$

In order to find the eigenmodes, this can be rewritten into the form:

$$\frac{\sin(k\ell)\sin(Nq)(v+w\xi)}{w\sin(q)} + \sin(k\ell)\cos(Nq) = \varphi(f) = 0, \tag{2.79}$$

where it was used that $\xi = \cos(q)$.

This condition is not satisfied for any frequencies falling within the band gap, i.e., there are no edge modes, as shown in Fig. 2.7**(B)**.

(C) Finite locally periodic antisymmetric structure with open ends
The case under consideration is the finite locally periodic structure comprised of N cells with no step change from the cross-section S_A to S_B at the beginning, as shown in Fig. 2.6**(C)**. The transfer matrix $\mathbf{M}_{\mathrm{C}}$ of such a structure then takes the form using the $\mathbf{M}^N$ matrix of Eq. (2.56) as follows:

$$\mathbf{M}_{\mathrm{C}} = \mathbf{M}^N \left(\mathbf{M}^{(\uparrow)}\right)^{-1}, \tag{2.80}$$

thereby eliminating the transition between cross-sections at the first cell.

Considering the Dirichlet boundary conditions for open ends (i.e., $P(x = 0) = 0$ and $P(x = 2N\ell) = 0$), analogically to Eq. (2.68), we obtain:

$$(0) = \begin{pmatrix} 1 & 1 \end{pmatrix} \mathbf{M}_{\mathrm{C}} \begin{pmatrix} 1 \\ -1 \end{pmatrix}. \tag{2.81}$$

From this, we get that

$$0 = (a - a^* + b^* - b)\frac{w\sin(Nq)}{v\sin(q)} = \frac{\mathrm{j}(v+w)\sin(2k\ell)\sin(Nq)}{v\sin(q)}. \tag{2.82}$$

Solving this equation leads to the same form as in Eq. (2.63), or finding the roots of $\eta(f)$.

(D) Finite locally periodic antisymmetric structure with closed ends
Finally, we consider the case for the structure corresponding to the transfer matrix $\mathbf{M}_{\mathrm{C}}$ (formulated in Eq. (2.80)), but its both ends are closed by a perfectly rigid wall, see Fig. 2.6**(D)**. Thus, it differs in the boundary conditions and we proceed analogously to Case **(B)**. The Neumann boundary conditions at the points $x = 0$ and $x = 2N\ell$ are satisfied by solving the following equation:

$$(0) = \begin{pmatrix} 1 & -1 \end{pmatrix} \mathbf{M}_{\mathrm{C}} \begin{pmatrix} 1 \\ 1 \end{pmatrix}. \tag{2.83}$$

After rearranging, we obtain that

$$0 = \frac{\sin(Nq)(a - a^* + b - b^*)}{\sin(q)} = \frac{\mathrm{j}(v+w)\sin(2k\ell)\sin(Nq)}{v\sin(q)}. \tag{2.84}$$

Employing the notation from Eq. (2.62), we obtain as follows:

$$\frac{\sin(2k\ell)\sin(Nq)}{\sin(q)} = \eta(f) = 0. \tag{2.85}$$

Using the resulting equation, we find the eigenmodes for the considered case. We see that this problem is a direct analogue of Eq. (2.62). The desired eigenmodes are shown in Fig. 2.5.

By using the derived relationships, we can also examine the transmission properties of a multi-cell structure (see Fig. 2.8). We apply the Chebyshev identity to derive a general expression for the amplitude transmission coefficient $\mathcal{T}_N$ of the multi-cell structure employing the notation for $\mathbf{M}^N$ introduced in Eq. (2.54) in the following form [8]:

$$\mathcal{T}_N = \left(\frac{P_+(x = 2N\ell)}{P_+(x = 0)} \right)_{P_-(x=2N\ell)=0} = \frac{1}{a_N^*}. \tag{2.86}$$

The reflection coefficient is equal to:

$$\mathcal{R}_N = \left(\frac{P_-(x = 0)}{P_+(x = 0)} \right)_{P_-(x=2N\ell)=0} = -\frac{b_N^*}{a_N^*}. \tag{2.87}$$

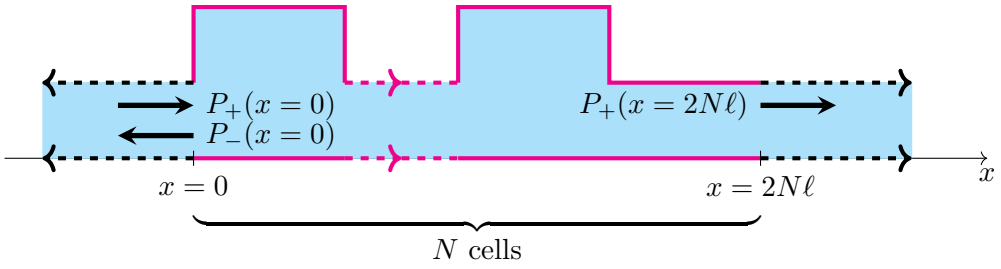

Fig. 2.8: A diagram of wave propagation through a multi-cell structure of length $2N\ell$ (marked in red).

Based on the law of conservation of energy, the following must be satisfied:

$$|\mathcal{T}_N|^2 + |\mathcal{R}_N|^2 = 1 \quad \Longrightarrow \quad \frac{1}{|a_N|^2} + \frac{|b_N|^2}{|a_N|^2} = 1. \tag{2.88}$$

It follows from the above:

$$1 + |b_N|^2 = |a_N|^2. \tag{2.89}$$

Thus it holds that

$$|\mathcal{T}_N|^2 = \frac{1}{|a_N|^2} = \frac{1}{1 + |b_N|^2}\ . \tag{2.90}$$

Substituting into Eq. (2.88) then gives the resulting form:

$$|\mathcal{T}_N|^2 = \frac{1}{1 + |b|^2 \left(\frac{\sin(Nq)}{\sin(q)} \right)^2} = \frac{1}{1 + \frac{(v^2 - w^2)^2 \sin^2(k\ell)}{4v^2 w^2} \left(\frac{\sin(Nq)}{\sin(q)} \right)^2}. \tag{2.91}$$

The transmission of the propagating waves for particular waveguides is shown in Fig. 2.9.

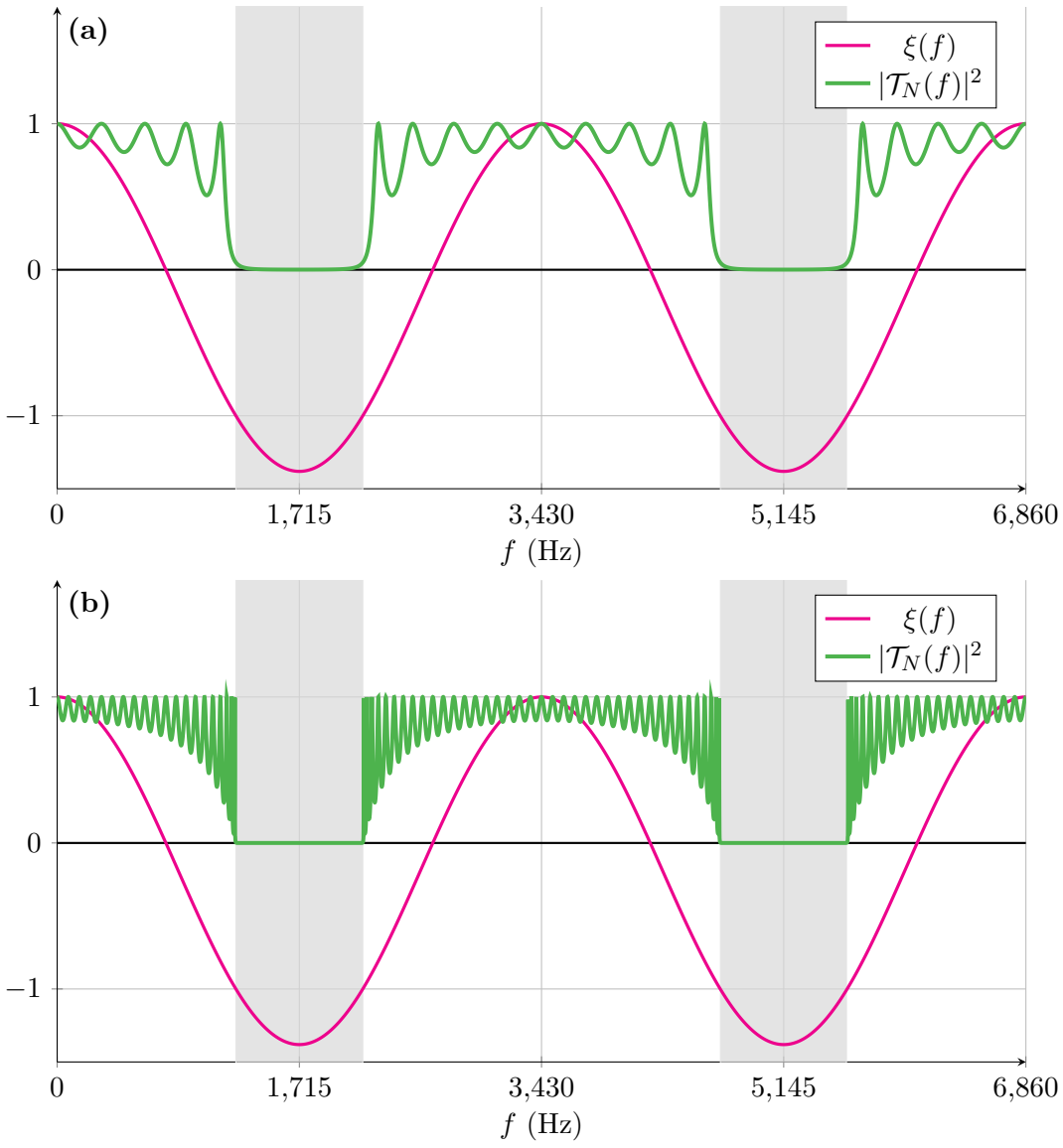

Fig. 2.9: The square of the modulus of the transmission coefficient $\mathcal{T}_N$ for particular locally periodic structures composed of N identical cells: **(a)** $N = 5$, **(b)** $N = 20$. Values of chosen parameters: $c_0 = 343$ ms^{-1}, $\ell = 0.05$ m, $f \in [0; 6{,}860]$ Hz, and $v = 0.3$. The gray region indicates the frequency range falling within the band gaps.

The TMM can also be expressed using the modified volume acoustic velocity and total pressure, which can be advantageous for the application of the Dirichlet and Neumann boundary conditions. We now show how this can be achieved.
After substituting $u(x,t)$ and $p'(x,t)$ into the Euler equation (2.9), we obtain the following form:

$$-\mathrm{j}\rho_0\omega U(x) = -\frac{\mathrm{d}P(x)}{\mathrm{d}x}. \tag{2.92}$$

We modify this equation as follows:

$$\mathrm{j}\rho_0\omega W_v(x) = v\frac{\mathrm{d}P(x)}{\mathrm{d}x}, \tag{2.93}$$

and

$$\mathrm{j}\rho_0\omega W_w(x) = w\frac{\mathrm{d}P(x)}{\mathrm{d}x}, \tag{2.94}$$

employing the coupling coefficients v and w, where

$$W_v(x) = vU(x), \tag{2.95}$$

and

$$W_w(x) = wU(x), \tag{2.96}$$

are the modified volume acoustic velocities.

Given the solution of the Helmholtz equation and its derivative (expressed in Eq. (2.71)), the following relations valid for the individual cross sections from Eqs. (2.93) and (2.94) hold:

$$W_v(x) = -\frac{\mathrm{j}v}{\rho_0\omega}\frac{\mathrm{d}P(x)}{\mathrm{d}x} = \frac{v}{Z}\left[P_+(x) - P_-(x)\right], \tag{2.97}$$

$$W_w(x) = -\frac{\mathrm{j}w}{\rho_0\omega}\frac{\mathrm{d}P(x)}{\mathrm{d}x} = \frac{w}{Z}\left[P_+(x) - P_-(x)\right], \tag{2.98}$$

where $Z = \rho_0 c_0$ is the acoustic impedance.
The relationships in Eqs. (2.97) and (2.98) can be expressed in matrix form as follows:

$$\begin{pmatrix} P(x) \\ W_v(x) \end{pmatrix} = \begin{pmatrix} 1 & 1 \\ \frac{v}{Z} & -\frac{v}{Z} \end{pmatrix} \begin{pmatrix} P_+(x) \\ P_-(x) \end{pmatrix} = \mathbf{M}_v^{(+)}\Psi(x), \tag{2.99}$$

$$\begin{pmatrix} P(x) \\ W_w(x) \end{pmatrix} = \begin{pmatrix} 1 & 1 \\ \frac{w}{Z} & -\frac{w}{Z} \end{pmatrix} \begin{pmatrix} P_+(x) \\ P_-(x) \end{pmatrix} = \mathbf{M}_w^{(+)}\Psi(x). \tag{2.100}$$

Similarly, the following relations for a wave propagating in the opposite direction can be written:

$$\begin{pmatrix} P(x) \\ W_v(x) \end{pmatrix} = \begin{pmatrix} 1 & 1 \\ -\frac{v}{Z} & \frac{v}{Z} \end{pmatrix} \begin{pmatrix} P_+(x) \\ P_-(x) \end{pmatrix} = \mathbf{M}_v^{(-)}\Psi(x), \tag{2.101}$$

$$\begin{pmatrix} P(x) \\ W_w(x) \end{pmatrix} = \begin{pmatrix} 1 & 1 \\ -\frac{w}{Z} & \frac{w}{Z} \end{pmatrix} \begin{pmatrix} P_+(x) \\ P_-(x) \end{pmatrix} = \mathbf{M}_w^{(-)}\Psi(x). \tag{2.102}$$

The various types of finite locally periodic structure from Fig. 2.6 can also be solved in a way that expresses the total acoustic pressure and the total modified volume acoustic velocity.

(A) Finite locally periodic symmetric structure with open ends

Considering the structure previously analysed in Case **(A)**, we employ the transfer matrix $\mathbf{M}_{\mathrm{A}}$ from Eq. (2.67) as follows:

$$\begin{pmatrix} P\left[(2N+1)\ell\right] \\ W_w\left[(2N+1)\ell\right] \end{pmatrix} = \mathbf{M}_w^{(+)} \mathbf{M}_{\mathrm{A}} \left(\mathbf{M}_w^{(+)}\right)^{-1} \begin{pmatrix} P(0) \\ W_w(0) \end{pmatrix} = \hat{\mathbf{M}}^{(W)} \begin{pmatrix} P(0) \\ W_w(0) \end{pmatrix}. \tag{2.103}$$

The following boundary conditions for the considered structure with open ends must be met: $P\left[(2N+1)\ell\right] = P(0) = 0$, and the following equality holds:

$$\begin{pmatrix} 0 \\ W_w\left[(2N+1)\ell\right] \end{pmatrix} = \hat{\mathbf{M}}^{(W)} \begin{pmatrix} 0 \\ W_w(0) \end{pmatrix}. \tag{2.104}$$

We thus obtain that

$$\hat{M}_{12}^{(W)} = 0, \tag{2.105}$$

and that can be expressed as:

$$\frac{\mathrm{j}Z\sin(k\ell)\{w\sin(Nq) + v\sin[(N+1)q]\}}{vw\sin(q)} = 0 \quad \Longrightarrow \quad \nu(f) = 0, \tag{2.106}$$

where $\nu(f)$ was introduced in Eq. (2.70). We thus obtain the same results also by employing the volume acoustic velocity for Case **(A)**.

(B) Finite locally periodic symmetric structure with closed ends

We start from Eq. (2.103), but apply different boundary conditions. The ends of the locally periodic structure are closed by a perfectly rigid wall, thus the condition must hold that $W_v[(2N+1)\ell] = W_w(0) = 0$. Applying this, we obtain:

$$\begin{pmatrix} P[(2N+1)\ell] \\ 0 \end{pmatrix} = \hat{\mathbf{M}}^{(W)} \begin{pmatrix} P(0) \\ 0 \end{pmatrix}. \tag{2.107}$$

From here, it is evident that the following equation must hold:

$$\hat{M}_{21}^{(W)} = 0. \tag{2.108}$$

And we can write that

$$\frac{\mathrm{j}\sin(k\ell)\{v\sin(Nq) + w\sin[(N+1)q]\}}{Z\sin(q)} = 0 \quad \Longrightarrow \quad \varphi(f) = 0, \tag{2.109}$$

where $\varphi(f)$ was introduced in Eq. (2.79). Also this result is identical to the form derived in the previous text.

(C) Finite locally periodic antisymmetric structure with open ends

For Case **(C)**, we proceed similarly as in the previous text employing the total transfer matrix $\mathbf{M}_{\mathrm{C}}$ formulated in Eq. (2.80) as:

$$\begin{pmatrix} P(2N\ell) \\ W_v(2N\ell) \end{pmatrix} = \mathbf{M}_v^{(+)} \mathbf{M}_{\mathrm{C}} \left(\mathbf{M}_w^{(+)}\right)^{-1} \begin{pmatrix} P(0) \\ W_w(0) \end{pmatrix} = \mathbf{M}^{(W)} \begin{pmatrix} P(0) \\ W_w(0) \end{pmatrix}. \tag{2.110}$$

Also here, it must hold that the ends of the locally periodic structure are open, we can write that $P(2N\ell) = P(0) = 0$, thus

$$\begin{pmatrix} 0 \\ W_v(2N\ell) \end{pmatrix} = \mathbf{M}^{(W)} \begin{pmatrix} 0 \\ W_w(0) \end{pmatrix}. \tag{2.111}$$

From this, we obtain:

$$M_{12}^{(W)} = 0. \tag{2.112}$$

This can be formulated as:

$$\frac{Z \sin(Nq)(a - a^* - b + b^*)}{2v \sin(q)} = 0 \quad \Longrightarrow \quad \frac{\sin(2k\ell)\sin(Nq)}{\sin(q)} = \eta(f) = 0. \tag{2.113}$$

It can be seen that finding bulk and edge modes (roots of $\eta(f)$) in Eq. (2.113) corresponds to the result already derived in this section. This is shown in Fig. 2.5.

(D) Finite locally periodic antisymmetric structure with closed ends

Finally, we start from Eq. (2.110), but apply different boundary conditions. The ends of the locally periodic structure are closed by a perfectly rigid wall, thus the condition must hold that $W_v(2N\ell) = W_w(0) = 0$. Applying this, we obtain:

$$\begin{pmatrix} P(2N\ell) \\ 0 \end{pmatrix} = \mathbf{M}^{(W)} \begin{pmatrix} P(0) \\ 0 \end{pmatrix}. \tag{2.114}$$

From here, it is evident that the following equation must hold:

$$M_{21}^{(W)} = 0. \tag{2.115}$$

And we can write that

$$\frac{v \sin(Nq)(a - a^* + b - b^*)}{2Z \sin(q)} = 0 \quad \Longrightarrow \quad \frac{\sin(2k\ell)\sin(Nq)}{\sin(q)} = \eta(f) = 0. \tag{2.116}$$

This yields the same results as in Case **(D)** analysed previously in this section.

Chapter 3

One-dimensional Su-Schrieffer-Heeger (SSH) model

The one-dimensional version of the Su-Schrieffer-Heeger (SSH) model constitutes the most elementary instance of a nontrivial topological system.
This model consists of a one-dimensional chain of two different "atoms" (A and B) with periodically alternating coupling coefficients v and w between the nearest neighbors. A cell of width a in the 1D chain is chosen so that v is an intrinsic parameter and the cell has inversion symmetry with respect to its center, see Fig. 3.1**(b)**. The circles represent two different atoms arranged in alternating order.

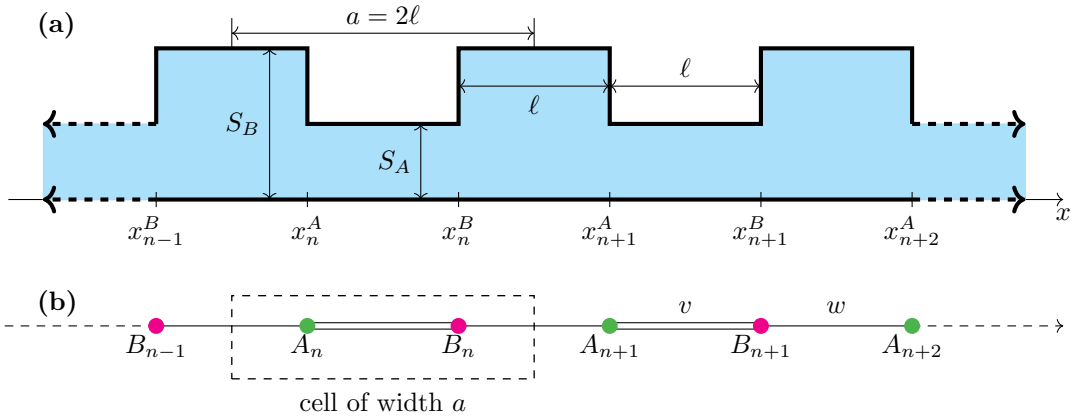

Fig. 3.1: **(a)** A diagram of a 2D acoustic waveguide as an infinite periodic structure with edges from the area S_A to S_B and vice versa. **(b)** The explicit mapping to the SSH discrete model is depicted.

The corresponding Hamiltonian matrix [7] can be written as:

$$\boldsymbol{H} = \begin{pmatrix} 0 & \hat{h}(q) \\ \hat{h}^*(q) & 0 \end{pmatrix}, \tag{3.1}$$

where

$$\hat{h}(q) = v + we^{\mathrm{j}q}, \tag{3.2}$$

and the dimensionless Bloch wave number $q = \mu a$. To denote the Bloch wave number we use μ and a is the spatial period.
The ratio v/w determines whether the system will have an open or closed band gap. If $v/w \neq 1$, then the system has an open band gap, and if $v/w = 1$, then the system has a closed band gap

at the edges of the Brillouin zone[1]. We discuss this further in Section 3.2.

3.1 Derivation of SSH Model Using TMM

The solution to the corresponding Helmholtz equation (2.5) can be written for the designated regions of the waveguide shown in Fig. 3.2 as follows:

Region I

$$P^{(\mathrm{I})}(x) = P_{+}^{(\mathrm{I})}(x) + P_{-}^{(\mathrm{I})}(x) = Ae^{\mathrm{j}kx} + Be^{-\mathrm{j}kx}, \quad x_{n-1}^{B} \leq x \leq x_{n}^{A}. \tag{3.3}$$

$$\Psi^{(\mathrm{I})}(x) = \begin{pmatrix} P_{+}^{(\mathrm{I})}(x) \\ P_{-}^{(\mathrm{I})}(x) \end{pmatrix} = \begin{pmatrix} Ae^{\mathrm{j}kx} \\ Be^{-\mathrm{j}kx} \end{pmatrix}. \tag{3.4}$$

Region II

$$P^{(\mathrm{II})}(x) = P_{+}^{(\mathrm{II})}(x) + P_{-}^{(\mathrm{II})}(x) = Fe^{\mathrm{j}kx} + Ge^{-\mathrm{j}kx}, \quad x_{n}^{A} \leq x \leq x_{n}^{B}. \tag{3.5}$$

$$\Psi^{(\mathrm{II})}(x) = \begin{pmatrix} P_{+}^{(\mathrm{II})}(x) \\ P_{-}^{(\mathrm{II})}(x) \end{pmatrix} = \begin{pmatrix} Fe^{\mathrm{j}kx} \\ Ge^{-\mathrm{j}kx} \end{pmatrix}. \tag{3.6}$$

Region III

$$P^{(\mathrm{III})}(x) = P_{+}^{(\mathrm{III})}(x) + P_{-}^{(\mathrm{III})}(x) = Ce^{\mathrm{j}kx} + De^{-\mathrm{j}kx}, \quad x_{n}^{B} \leq x \leq x_{n+1}^{A}. \tag{3.7}$$

$$\Psi^{(\mathrm{III})}(x) = \begin{pmatrix} P_{+}^{(\mathrm{III})}(x) \\ P_{-}^{(\mathrm{III})}(x) \end{pmatrix} = \begin{pmatrix} Ce^{\mathrm{j}kx} \\ De^{-\mathrm{j}kx} \end{pmatrix}. \tag{3.8}$$

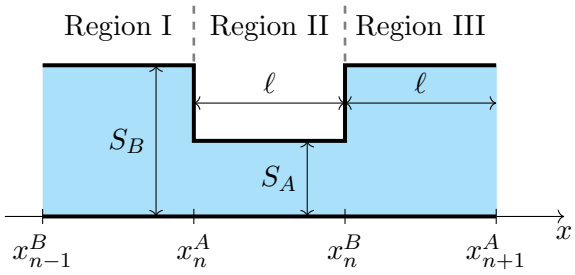

Fig. 3.2: A diagram of the considered cell with designated Regions I, II and III.

[1]The Brillouin zone is a fundamental concept in the theory of the electronic band structure in solids and is used to describe permissible states of electrons in a crystal lattice. Simply put, it is a geometric way of understanding how electrons can move in a solid. Analogously, it can be applied to other systems where the role of electron wave functions is played by, for instance, acoustic or elastic waves.

We introduce the notation of points on the x-axis (x^A and x^B) to emulate a diatomic system with tight binding. Employing the already introduced matrices (Eqs. (2.19), (2.27) and (2.33)), we express the transfer matrix from the point x_{n-1}^B to the point x_n^A as

$$\Psi^{(\mathrm{II})}\left(x_n^A\right) = \mathbf{M}^{(\downarrow)}\mathbf{M}^{(\rightarrow)}\Psi^{(\mathrm{I})}\left(x_{n-1}^B\right). \tag{3.9}$$

Considering the equality (2.100), we get that

$$\begin{pmatrix} P^{(\mathrm{II})}\left(x_n^A\right) \\ W_v^{(\mathrm{II})}\left(x_n^A\right) \end{pmatrix} = \mathbf{M}_v^{(+)}\mathbf{M}^{(\downarrow)}\mathbf{M}^{(\rightarrow)}\left(\mathbf{M}_w^{(+)}\right)^{-1}\begin{pmatrix} P^{(\mathrm{I})}\left(x_{n-1}^B\right) \\ W_w^{(\mathrm{I})}\left(x_{n-1}^B\right) \end{pmatrix} = \\ \begin{pmatrix} \cos(k\ell) & \frac{\mathrm{j}Z\sin(k\ell)}{w} \\ \frac{\mathrm{j}w\sin(k\ell)}{Z} & \cos(k\ell) \end{pmatrix}\begin{pmatrix} P^{(\mathrm{I})}\left(x_{n-1}^B\right) \\ W_w^{(\mathrm{I})}\left(x_{n-1}^B\right) \end{pmatrix} = \begin{pmatrix} a_w^{(+)} & b_w^{(+)} \\ c_w^{(+)} & d_w^{(+)} \end{pmatrix}\begin{pmatrix} P^{(\mathrm{I})}\left(x_{n-1}^B\right) \\ W_w^{(\mathrm{I})}\left(x_{n-1}^B\right) \end{pmatrix}. \tag{3.10}$$

Assuming a wave propagating from the point x_n^B to the point x_n^A, we can write that

$$\Psi^{(\mathrm{I})}\left(x_n^A\right) = \mathbf{M}^{(\uparrow)}\mathbf{M}^{(\rightarrow)}\Psi^{(\mathrm{II})}\left(x_n^B\right), \tag{3.11}$$

and the corresponding transfer matrix can be expressed as follows:

$$\begin{pmatrix} P^{(\mathrm{I})}\left(x_n^A\right) \\ W_w^{(\mathrm{I})}\left(x_n^A\right) \end{pmatrix} = \mathbf{M}_w^{(-)}\mathbf{M}^{(\uparrow)}\mathbf{M}^{(\rightarrow)}\left(\mathbf{M}_v^{(-)}\right)^{-1}\begin{pmatrix} P^{(\mathrm{II})}\left(x_n^B\right) \\ W_v^{(\mathrm{II})}\left(x_n^B\right) \end{pmatrix} = \\ \begin{pmatrix} \cos(k\ell) & -\frac{\mathrm{j}Z\sin(k\ell)}{v} \\ -\frac{\mathrm{j}v\sin(k\ell)}{Z} & \cos(k\ell) \end{pmatrix}\begin{pmatrix} P^{(\mathrm{II})}\left(x_n^B\right) \\ W_v^{(\mathrm{II})}\left(x_n^B\right) \end{pmatrix} = \begin{pmatrix} a_v^{(-)} & b_v^{(-)} \\ c_v^{(-)} & d_v^{(-)} \end{pmatrix}\begin{pmatrix} P^{(\mathrm{II})}\left(x_n^B\right) \\ W_v^{(\mathrm{II})}\left(x_n^B\right) \end{pmatrix}. \tag{3.12}$$

From Eqs. (3.10) and (3.12), we express that

$$W_v^{(\mathrm{II})}\left(x_n^A\right) = \frac{d_w^{(+)}}{b_w^{(+)}}P^{(\mathrm{II})}\left(x_n^A\right) + \left(c_w^{(+)} - \frac{a_w^{(+)}d_w^{(+)}}{b_w^{(+)}}\right)P^{(\mathrm{I})}\left(x_{n-1}^B\right) = \\ \frac{a_w^{(+)}}{b_w^{(+)}}P^{(\mathrm{II})}\left(x_n^A\right) - \frac{1}{b_w^{(+)}}P^{(\mathrm{I})}\left(x_{n-1}^B\right), \tag{3.13}$$

$$W_w^{(\mathrm{I})}\left(x_n^A\right) = \frac{d_v^{(-)}}{b_v^{(-)}}P^{(\mathrm{I})}\left(x_n^A\right) + \left(c_v^{(-)} - \frac{a_v^{(-)}d_v^{(-)}}{b_v^{(-)}}\right)P^{(\mathrm{II})}\left(x_n^B\right) = \\ \frac{a_v^{(-)}}{b_v^{(-)}}P^{(\mathrm{I})}\left(x_n^A\right) - \frac{1}{b_v^{(-)}}P^{(\mathrm{II})}\left(x_n^B\right), \tag{3.14}$$

where we used that $a_w^{(+)} = d_w^{(+)}$ and $a_v^{(-)} = d_v^{(-)}$.
At the point x_n^A, the following equality between the volume velocities holds:

$$W_v^{(\mathrm{II})}\left(x_n^A\right) = W_w^{(\mathrm{I})}\left(x_n^A\right), \tag{3.15}$$

and we also note that

$$P^{(\mathrm{I})}\left(x_n^A\right) = P^{(\mathrm{II})}\left(x_n^A\right) = P\left(x_n^A\right). \tag{3.16}$$

By substituting Eqs. (3.13) and (3.14) into Eq. (3.15), we obtain:

$$-w\left[\cos(k\ell)P\left(x_n^A\right)-P\left(x_{n-1}^B\right)\right]=v\left[\cos(k\ell)P\left(x_n^A\right)-P\left(x_n^B\right)\right]. \tag{3.17}$$

This can be simplified to the following equation:

$$vP\left(x_n^B\right)+wP\left(x_{n-1}^B\right)=(v+w)\cos(k\ell)P\left(x_n^A\right)=\cos(k\ell)P\left(x_n^A\right). \tag{3.18}$$

In an analogous way (actually the inverse procedure) we find the transfer matrix for a wave propagating from the point x_n^A to the point x_n^B:

$$\Psi^{(\mathrm{III})}\left(x_n^B\right)=\mathbf{M}^{(\uparrow)}\mathbf{M}^{(\rightarrow)}\Psi^{(\mathrm{II})}\left(x_n^A\right), \tag{3.19}$$

and we can write that

$$\begin{pmatrix}P^{(\mathrm{III})}\left(x_n^B\right)\\W_w^{(\mathrm{III})}\left(x_n^B\right)\end{pmatrix}=\mathbf{M}_w^{(+)}\mathbf{M}^{(\uparrow)}\mathbf{M}^{(\rightarrow)}\left(\mathbf{M}_v^{(+)}\right)^{-1}\begin{pmatrix}P^{(\mathrm{II})}\left(x_n^A\right)\\W_v^{(\mathrm{II})}\left(x_n^A\right)\end{pmatrix}=$$
$$\begin{pmatrix}\cos(k\ell)&\frac{\mathrm{j}Z\sin(k\ell)}{v}\\\frac{\mathrm{j}v\sin(k\ell)}{Z}&\cos(k\ell)\end{pmatrix}\begin{pmatrix}P^{(\mathrm{II})}\left(x_n^A\right)\\W_v^{(\mathrm{II})}\left(x_n^A\right)\end{pmatrix}=\begin{pmatrix}a_v^{(+)}&b_v^{(+)}\\c_v^{(+)}&d_v^{(+)}\end{pmatrix}\begin{pmatrix}P^{(\mathrm{II})}\left(x_n^A\right)\\W_v^{(\mathrm{II})}\left(x_n^A\right)\end{pmatrix}. \tag{3.20}$$

Similarly, we can find the transfer matrix for a wave propagating from the point x_{n+1}^A to the point x_n^B:

$$\Psi^{(\mathrm{II})}\left(x_n^B\right)=\mathbf{M}^{(\downarrow)}\mathbf{M}^{(\rightarrow)}\Psi^{(\mathrm{III})}\left(x_{n+1}^A\right), \tag{3.21}$$

and in matrix form, we express this as:

$$\begin{pmatrix}P^{(\mathrm{II})}\left(x_n^B\right)\\W_v^{(\mathrm{II})}\left(x_n^B\right)\end{pmatrix}=\mathbf{M}_v^{(-)}\mathbf{M}^{(\downarrow)}\mathbf{M}^{(\rightarrow)}\left(\mathbf{M}_w^{(-)}\right)^{-1}\begin{pmatrix}P^{(\mathrm{III})}\left(x_{n+1}^A\right)\\W_w^{(\mathrm{III})}\left(x_{n+1}^A\right)\end{pmatrix}=$$
$$\begin{pmatrix}\cos(k\ell)&-\frac{\mathrm{j}Z\sin(k\ell)}{w}\\-\frac{\mathrm{j}w\sin(k\ell)}{Z}&\cos(k\ell)\end{pmatrix}\begin{pmatrix}P^{(\mathrm{III})}\left(x_{n+1}^A\right)\\W_w^{(\mathrm{III})}\left(x_{n+1}^A\right)\end{pmatrix}=\begin{pmatrix}a_w^{(-)}&b_w^{(-)}\\c_w^{(-)}&d_w^{(-)}\end{pmatrix}\begin{pmatrix}P^{(\mathrm{III})}\left(x_{n+1}^A\right)\\W_w^{(\mathrm{III})}\left(x_{n+1}^A\right)\end{pmatrix}. \tag{3.22}$$

From Eqs. (3.20) and (3.22), we can write that

$$W_w^{(\mathrm{III})}\left(x_n^B\right)=\frac{d_v^{(+)}}{b_v^{(+)}}P^{(\mathrm{III})}\left(x_n^B\right)+\left(c_v^{(+)}-\frac{a_v^{(+)}d_v^{(+)}}{b_v^{(+)}}\right)P^{(\mathrm{II})}\left(x_n^A\right)=$$
$$\frac{a_v^{(+)}}{b_v^{(+)}}P^{(\mathrm{III})}\left(x_n^B\right)-\frac{1}{b_v^{(+)}}P^{(\mathrm{II})}\left(x_n^A\right), \tag{3.23}$$

$$W_v^{(\mathrm{II})}\left(x_n^B\right)=\frac{d_w^{(-)}}{b_w^{(-)}}P^{(\mathrm{II})}\left(x_n^B\right)+\left(c_w^{(-)}-\frac{a_w^{(-)}d_w^{(-)}}{b_w^{(-)}}\right)P^{(\mathrm{III})}\left(x_{n+1}^A\right)=$$
$$\frac{a_w^{(-)}}{b_w^{(-)}}P^{(\mathrm{II})}\left(x_n^B\right)-\frac{1}{b_w^{(-)}}P^{(\mathrm{III})}\left(x_{n+1}^A\right). \tag{3.24}$$

At the point x_n^B, the following equality between the volume velocities holds:

$$W_w^{(\mathrm{III})}\left(x_n^B\right) = W_v^{(\mathrm{II})}\left(x_n^B\right), \tag{3.25}$$

and we also note that

$$P^{(\mathrm{II})}\left(x_n^B\right) = P^{(\mathrm{III})}\left(x_n^B\right) = P\left(x_n^B\right). \tag{3.26}$$

By substituting Eqs. (3.23) and (3.24) into Eq. (3.25), we obtain:

$$v\left[P\left(x_n^A\right) - \cos(k\ell)P\left(x_n^B\right)\right] = w\left[\cos(k\ell)P\left(x_n^B\right) - P\left(x_{n+1}^A\right)\right], \tag{3.27}$$

We simplify this equation as follows:

$$wP\left(x_{n+1}^A\right) + vP\left(x_n^A\right) = (v+w)\cos(k\ell)P\left(x_n^B\right) = \cos(k\ell)P\left(x_n^B\right). \tag{3.28}$$

We now restate Eqs. (3.18) and (3.28), and introduce a new notation for clarity:

$$\boxed{vB_n + wB_{n-1} = E(k)A_n,} \tag{3.29}$$

$$\boxed{wA_{n+1} + vA_n = E(k)B_n,} \tag{3.30}$$

where $E(k) = \cos(k\ell)$, $A_n = P\left(x_n^A\right)$, and $B_n = P\left(x_n^B\right)$.

The SSH model [11] corresponding to the formulation of the time-independent Schrödinger equation for stationary states and for the diatomic system with tight binding is thus expressed in Eqs. (3.29) and (3.30). The originally continuous system is thereby transformed into a discrete one.

3.2 Infinite Structure

Considering an infinite waveguide, we can express the eigenvalue problem based on Eqs. (3.29) and (3.30) (the SSH model) as follows:

$$\mathbf{H}\boldsymbol{X} = E(k)\boldsymbol{X}, \tag{3.31}$$

where

$$\mathbf{H} = \begin{pmatrix} \ddots & \ddots & & & & & \\ \ddots & 0 & v & & & & \\ & v & 0 & w & & & \\ & & w & 0 & v & & \\ & & & v & 0 & \ddots & \\ & & & & \ddots & \ddots & \end{pmatrix}, \tag{3.32}$$

and

$$\boldsymbol{X} = (\dots, A_n, B_n, \dots)^{\intercal}. \tag{3.33}$$

From here, it can be observed that $E(k)$ can be regarded as a kind of "acoustic eigenenergy". The eigen-wave numbers k can be found directly from the obtained eigenvalues $E(k)$ of the Hermitian matrix $\mathbf{H}$. That means, $\mathbf{H}$ is a transposed complex conjugate matrix to itself, also denoted as $\mathbf{H}^{\dagger} = \mathbf{H}$.

Taking into account that the analysed waveguide represents an infinite periodic structure, it is advantageous to employ the Bloch-Floquet theorem.
Based on this theorem, it holds that the amplitude of the acoustic pressure (Bloch function or Bloch wave) at the position x of the infinite periodic structure (waveguide) can be expressed as [20]:

$$P_{\pm}(x) = e^{\pm \mathrm{j}\mu x}\mathcal{P}_{\pm}(x) = e^{\pm \mathrm{j}\frac{q}{a}x}\mathcal{P}_{\pm}(x), \tag{3.34}$$

where μ is the Bloch wave number, $q = \mu a$ is the dimensionless Bloch wave number and $\mathcal{P}_{\pm}(x)$ is a periodic function with the spatial period a of the given structure, i.e.,

$$\mathcal{P}_{\pm}(x + a) = \mathcal{P}_{\pm}(x). \tag{3.35}$$

$P_{\pm}$ represents two linearly independent solutions (Bloch waves). P_{+} is associated with the positive sign of the Bloch wave number, while P_{-} is associated with the negative sign of the Bloch wave number. In the next part of the text, both lower and upper indices are employed for the used symbols implying this convention.
Consequently, we can express the solutions for the infinite waveguide under consideration as a linear combination of these Bloch functions as follows:

$$P(x) = \alpha P_{+}(x) + \beta P_{-}(x), \tag{3.36}$$

where α, β are integration constants that we determine from boundary conditions.
Using Eq. (3.34), it holds that

$$P_{\pm}(x + a) = e^{\pm \mathrm{j}\frac{q}{a}(x+a)}\mathcal{P}_{\pm}(x + a). \tag{3.37}$$

Employing Eqs. (3.34) and (3.35), we obtain:

$$P_{\pm}(x+a) = e^{\pm \mathrm{j}\frac{q}{a}(x+a)}\mathcal{P}_{\pm}(x+a) = e^{\pm \mathrm{j}\frac{q}{a}(x+a)}\mathcal{P}_{\pm}(x) = e^{\pm \mathrm{j}q}\underbrace{e^{\pm \mathrm{j}\frac{q}{a}x}\mathcal{P}_{\pm}(x)}_{=P_{\pm}(x)}. \tag{3.38}$$

From here, we can write that

$$P_{\pm}(x+a) = e^{\pm \mathrm{j}q}P_{\pm}(x). \tag{3.39}$$

The relation expressed in Eq. (3.39) is referred to as the Bloch condition.
Without loss of generality, the Bloch condition can be represented in the following form:

$$P_{\pm}\left(x - x_0^A + a\right) = e^{\pm \mathrm{j}q}P_{\pm}\left(x - x_0^A\right). \tag{3.40}$$

For $x = x_0^A$, we obtain using the Bloch condition (3.39):

$$A_1^{(\pm)} = P_{\pm}(a) = e^{\pm \mathrm{j}q}P_{\pm}(0) \equiv \mathcal{A}^{(\pm)}e^{\pm \mathrm{j}q}, \tag{3.41}$$

where x_0^A corresponds to the location of an edge of the considered waveguide (from a larger area to a smaller one, i.e., $S_B \to S_A$).
Again, employing the Bloch condition and Eq. (3.41), we can write that

$$A_2^{(\pm)} = P_{\pm}(2a) = e^{\pm \mathrm{j}q}P_{\pm}(a) = e^{\pm \mathrm{j}q}\mathcal{A}^{(\pm)}e^{\pm \mathrm{j}q} = \mathcal{A}^{(\pm)}e^{\pm \mathrm{j}2q}. \tag{3.42}$$

From here, it holds that

$$\boxed{A_n^{(\pm)} = \mathcal{A}^{(\pm)}e^{\pm \mathrm{j}nq}.} \tag{3.43}$$

Similarly, for the Bloch condition, we can express that

$$P_{\pm}\left(x - x_0^B + a\right) = e^{\mathrm{j}q}P_{\pm}\left(x - x_0^B\right). \tag{3.44}$$

Analogically, for $x = x_0^B$, where x_0^B corresponds to the location of an edge (from a smaller area to a larger one, i.e., $S_A \to S_B$) we obtain:

$$B_1^{(\pm)} = P_{\pm}(a) = e^{\pm \mathrm{j}q}P_{\pm}(0) \equiv \mathcal{B}^{(\pm)}e^{\pm \mathrm{j}q}. \tag{3.45}$$

Following the same procedure, we can write as follows:

$$\boxed{B_n^{(\pm)} = \mathcal{B}^{(\pm)}e^{\pm \mathrm{j}nq}.} \tag{3.46}$$

Using Eq. (3.36), we can write that

$$P(x_n^A) \equiv A_n = \alpha A_n^{(+)} + \beta A_n^{(-)}, \tag{3.47}$$

and

$$P(x_n^B) \equiv B_n = \alpha B_n^{(+)} + \beta B_n^{(-)}. \tag{3.48}$$

Substituting Eq. (3.47) and (3.48) into the SSH model (expressed in Eqs. (3.29) and (3.30)), we obtain:

$$v\left(\alpha B_n^{(+)} + \beta B_n^{(-)}\right) + w\left(\alpha B_{n-1}^{(+)} + \beta B_{n-1}^{(-)}\right) = E(k)\left(\alpha A_n^{(+)} + \beta A_n^{(-)}\right), \tag{3.49}$$

$$w\left(\alpha A_{n+1}^{(+)}+\beta A_{n+1}^{(-)}\right)+v\left(\alpha A_{n}^{(+)}+\beta A_{n}^{(-)}\right)=E(k)\left(\alpha B_{n}^{(+)}+\beta B_{n}^{(-)}\right)\ . \tag{3.50}$$

Employing Eqs. (3.49) and (3.50), the following equations hold:

$$vB_{n}^{(+)}+wB_{n-1}^{(+)}=E(k)A_{n}^{(+)}, \tag{3.51}$$

$$wA_{n+1}^{(+)}+vA_{n}^{(+)}=E(k)B_{n}^{(+)}, \tag{3.52}$$

$$vB_{n}^{(-)}+wB_{n-1}^{(-)}=E(k)A_{n}^{(-)}, \tag{3.53}$$

$$wA_{n+1}^{(-)}+vA_{n}^{(-)}=E(k)B_{n}^{(-)}. \tag{3.54}$$

After substituting Eqs. (3.43) and (3.46) into Eqs. (3.51)–(3.54) and algebraic manipulation, we arrive at the following matrix representations of the eigenvalue problem:

$$\underbrace{\begin{pmatrix}0 & v+we^{-\mathrm{j}q}\\ v+we^{\mathrm{j}q} & 0\end{pmatrix}}_{=\mathbf{H}^{(+)}}\begin{pmatrix}\mathcal{A}^{(+)}\\ \mathcal{B}^{(+)}\end{pmatrix}=E(k)\begin{pmatrix}\mathcal{A}^{(+)}\\ \mathcal{B}^{(+)}\end{pmatrix}, \tag{3.55}$$

$$\underbrace{\begin{pmatrix}0 & v+we^{\mathrm{j}q}\\ v+we^{-\mathrm{j}q} & 0\end{pmatrix}}_{=\mathbf{H}^{(-)}}\begin{pmatrix}\mathcal{A}^{(-)}\\ \mathcal{B}^{(-)}\end{pmatrix}=E(k)\begin{pmatrix}\mathcal{A}^{(-)}\\ \mathcal{B}^{(-)}\end{pmatrix}, \tag{3.56}$$

where $\mathbf{H}^{(+)}$ and $\mathbf{H}^{(-)}$ are Hermitian matrices (Bloch Hamiltonians).
The eigenvalues for $\mathbf{H}^{(+)}$ can be obtained by solving the following equation:

$$\det(\mathbf{H}^{(+)}-E\mathbf{I})=0, \tag{3.57}$$

where $\mathbf{I}$ is the identity matrix. Describing Eq. (3.57) in matrix form, we obtain:

$$\begin{vmatrix}-E & v+we^{-\mathrm{j}q}\\ v+we^{\mathrm{j}q} & -E\end{vmatrix}=0, \tag{3.58}$$

which is equal to solving the following equation:

$$E^{2}-\left(v+we^{\mathrm{j}q}\right)\left(v+we^{-\mathrm{j}q}\right)=0. \tag{3.59}$$

The solution of Eq. (3.59) yields two eigenvalues:

$$\boxed{E(k)=\cos(k\ell)=\pm\sqrt{v^{2}+w^{2}+2vw\cos(q)}=\pm\left|v+we^{\mathrm{j}q}\right|=E_{\pm}(q),} \tag{3.60}$$

and that coincides with the relationship formulated in Eq. (2.49).
We note that Eq. (3.60) represents a dispersion relation, see Fig. 3.3. The crossing of two bands of the SSH model at $v=w$ occurs precisely in the case of a trivial waveguide with constant cross section, as shown in Fig. 3.3**(b)**.
Following the same procedure for $\mathbf{H}^{(-)}$, it is obvious that solving $\det(\mathbf{H}^{(-)}-E\mathbf{I})=0$ leads to Eq. (3.59) and thus yields the same eigenvalues.

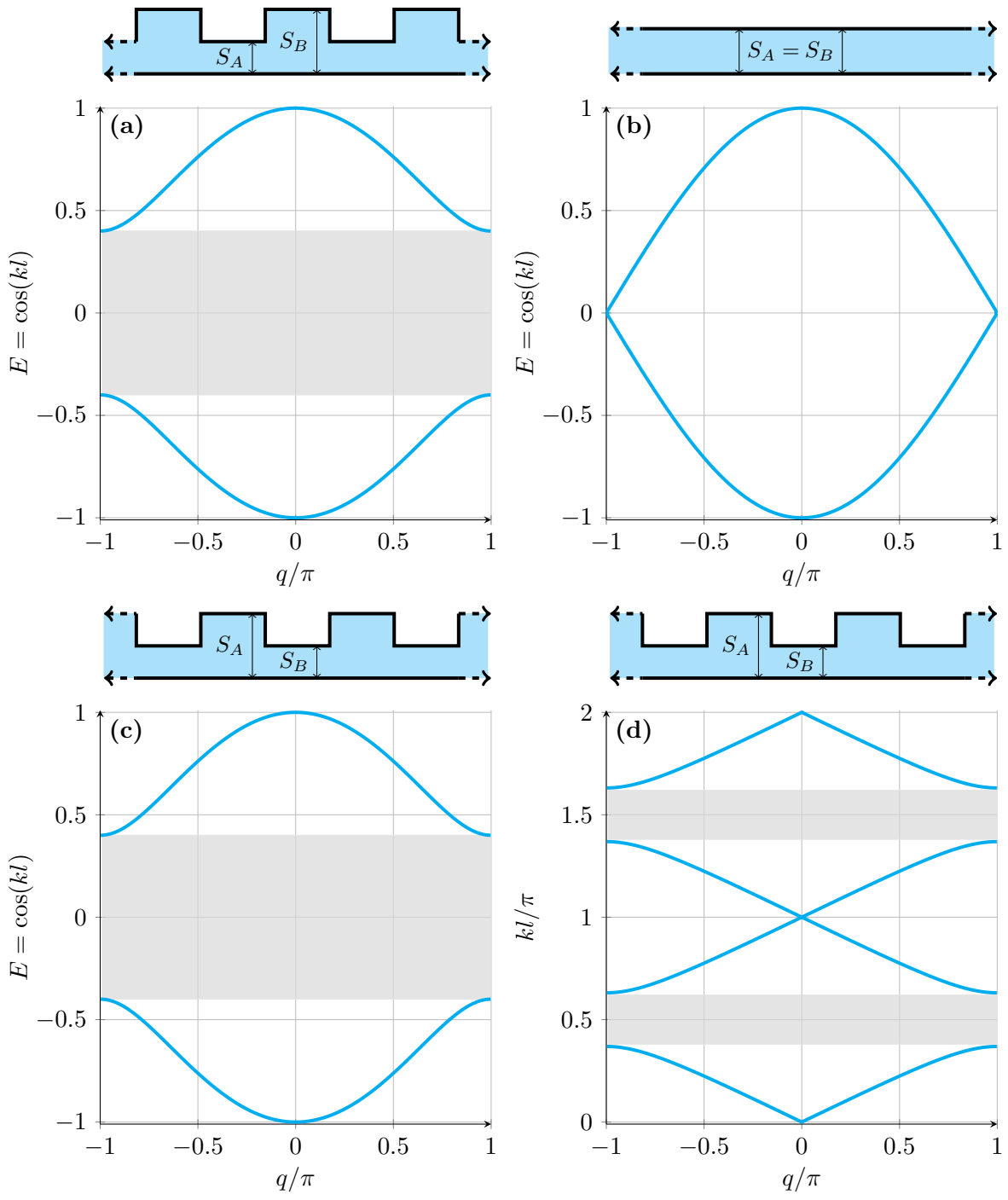

Fig. 3.3: The dispersion relation of the acoustic SSH model for three different values of the coupling coefficient v: **(a)** $v = 0.3$, **(b)** $v = 0.5$, and in **(c)** and **(d)**, $v = 0.7$. Note that **(d)** also corresponds with $v = 0.3$. The gray region indicates the band gaps.

For the eigenvalue $E_+(q) = \left|v + we^{\mathrm{j}q}\right|$, we find the eigenvector by solving the following system of two equations:

$$\begin{pmatrix} 0 & v + we^{-\mathrm{j}q} \\ v + we^{\mathrm{j}q} & 0 \end{pmatrix} \begin{pmatrix} \mathcal{A}^{(+)} \\ \mathcal{B}^{(+)} \end{pmatrix} = \left|v + we^{\mathrm{j}q}\right| \begin{pmatrix} \mathcal{A}^{(+)} \\ \mathcal{B}^{(+)} \end{pmatrix}, \tag{3.61}$$

which can be rewritten as:

$$\left(v + we^{-\mathrm{j}q}\right) \mathcal{B}^{(+)} = \left|v + we^{\mathrm{j}q}\right| \mathcal{A}^{(+)}, \tag{3.62}$$

$$\left(v + we^{\mathrm{j}q}\right) \mathcal{A}^{(+)} = \left|v + we^{\mathrm{j}q}\right| \mathcal{B}^{(+)}. \tag{3.63}$$

From here, using e.g. Eq. (3.62), we can write:

$$\mathcal{B}^{(+)} = \gamma \frac{\left|v + we^{\mathrm{j}q}\right|}{v + we^{-\mathrm{j}q}} = \gamma \frac{\left|v + we^{\mathrm{j}q}\right|}{\left|v + we^{-\mathrm{j}q}\right| e^{\mathrm{j}\phi(q)}} = \gamma e^{-\mathrm{j}\phi(q)}, \tag{3.64}$$

$$\mathcal{A}^{(+)} = \gamma, \tag{3.65}$$

where $\phi(q) = \arg\left(v + we^{-\mathrm{j}q}\right)$ and γ is an unknown constant.
By introducing $\theta(q) = \arg\left(v + we^{\mathrm{j}q}\right) = -\phi(q)$, the eigenvector can be expressed in the following form:

$$\boldsymbol{X}_+^{(+)} = \begin{pmatrix} \mathcal{A}^{(+)} \\ \mathcal{B}^{(+)} \end{pmatrix} = \gamma \begin{pmatrix} 1 \\ e^{\mathrm{j}\theta(q)} \end{pmatrix}. \tag{3.66}$$

Consequently, it holds that

$$\mathbf{H}^{(+)} \boldsymbol{X}_+^{(+)} = E_+ \boldsymbol{X}_+^{(+)}. \tag{3.67}$$

Analogically, we repeat the described procedure and determine the eigenvector of the eigenvalue $E_-(q) = -\left|v + we^{\mathrm{j}q}\right|$:

$$\boldsymbol{X}_-^{(+)} = \begin{pmatrix} \mathcal{A}^{(+)} \\ \mathcal{B}^{(+)} \end{pmatrix} = \gamma \begin{pmatrix} 1 \\ -e^{\mathrm{j}\theta(q)} \end{pmatrix}. \tag{3.68}$$

It can be easily verified that the eigenvectors (3.66) and (3.68) are mutually orthogonal:

$$\left(\boldsymbol{X}_+^{(+)}\right)^\dagger \boldsymbol{X}_-^{(+)} = 0. \tag{3.69}$$

Note that we could have equally expressed $\mathcal{A}^{(+)}$ from Eq. (3.62) and thus obtaining $\mathcal{A}^{(+)} = \gamma e^{-\mathrm{j}\theta(q)}$ and $\mathcal{B}^{(+)} = \gamma$. We would have expressed the found eigenvector as:

$$\tilde{\boldsymbol{X}}_+^{(+)} = \begin{pmatrix} \mathcal{A}^{(+)} \\ \mathcal{B}^{(+)} \end{pmatrix} = \gamma \begin{pmatrix} e^{-\mathrm{j}\theta(q)} \\ 1 \end{pmatrix}, \tag{3.70}$$

where the following relation holds for the eigenvectors:

$$\tilde{\boldsymbol{X}}_+^{(+)} = e^{-\mathrm{j}\theta(q)} \boldsymbol{X}_+^{(+)}. \tag{3.71}$$

We say that the eigenvector $\tilde{\boldsymbol{X}}_+^{(+)}$ is obtained through the gauge transformation of the eigenvector $\boldsymbol{X}_+^{(+)}$. Both of these eigenvectors are of equal quality; in other words, they are interchangeable.

Analogically, applying the gauge transformation on $\boldsymbol{X}_{-}^{(+)}$ yields the eigenvector $\tilde{\boldsymbol{X}}_{-}^{(+)}$.

Furthermore, it can be easily verified for the matrix operator $\mathbf{H}^{(-)}$ (which is the complex conjugate to the matrix operator $\mathbf{H}^{(+)}$) that the corresponding eigenvectors are also complex conjugates of eigenvectors (3.66) and (3.68):

$$\boldsymbol{X}_{+}^{(-)} = \begin{pmatrix} \mathcal{A}^{(-)} \\ \mathcal{B}^{(-)} \end{pmatrix} = \delta \begin{pmatrix} 1 \\ e^{-\mathrm{j}\theta(q)} \end{pmatrix}, \tag{3.72}$$

$$\boldsymbol{X}_{-}^{(-)} = \begin{pmatrix} \mathcal{A}^{(-)} \\ \mathcal{B}^{(-)} \end{pmatrix} = \delta \begin{pmatrix} 1 \\ -e^{-\mathrm{j}\theta(q)} \end{pmatrix}, \tag{3.73}$$

where δ is an unknown constant. Employing the gauge transformation, we obtain another representation of these eigenvectors as follows:

$$\tilde{\boldsymbol{X}}_{\pm}^{(-)} = e^{\mathrm{j}\theta(q)} \boldsymbol{X}_{\pm}^{(-)}. \tag{3.74}$$

Assume that $E(k) = E_{+} > 0$. Based on Eqs. (3.43), (3.46)-(3.48), (3.66), and (3.72), we can write:

$$\begin{aligned} \begin{pmatrix} A_n \\ B_n \end{pmatrix} = \begin{pmatrix} \alpha A_n^{(+)} + \beta A_n^{(-)} \\ \alpha B_n^{(+)} + \beta B_n^{(-)} \end{pmatrix} = \alpha \begin{pmatrix} A_n^{(+)} \\ B_n^{(+)} \end{pmatrix} + \beta \begin{pmatrix} A_n^{(-)} \\ B_n^{(-)} \end{pmatrix} = \\ \alpha e^{\mathrm{j}nq} \begin{pmatrix} \mathcal{A}^{(+)} \\ \mathcal{B}^{(+)} \end{pmatrix} + \beta e^{-\mathrm{j}nq} \begin{pmatrix} \mathcal{A}^{(-)} \\ \mathcal{B}^{(-)} \end{pmatrix} = \alpha\gamma e^{\mathrm{j}nq} \begin{pmatrix} 1 \\ e^{\mathrm{j}\theta(q)} \end{pmatrix} + \beta\delta e^{-\mathrm{j}nq} \begin{pmatrix} 1 \\ e^{-\mathrm{j}\theta(q)} \end{pmatrix}. \end{aligned} \tag{3.75}$$

Incorporating the constants γ and δ into α and β, we obtain the final desired relation:

$$\boxed{\begin{pmatrix} A_n \\ B_n \end{pmatrix} = \alpha e^{\mathrm{j}nq} \begin{pmatrix} 1 \\ e^{\mathrm{j}\theta(q)} \end{pmatrix} + \beta e^{-\mathrm{j}nq} \begin{pmatrix} 1 \\ e^{-\mathrm{j}\theta(q)} \end{pmatrix},} \tag{3.76}$$

where α and β are complex constants that need to be determined. Additionally, we recall that $\theta(q) = \arg\left(v + we^{\mathrm{j}q}\right)$.

Considering a system of semi-infinite length, also the Hermitian matrix (3.32) is semi-infinite. In order to express it, it is necessary to specify the boundary conditions (Dirichlet and Neumann), which then determine the behavior of such a system.
The use of semi-infinite systems leads us to consider so-called edge effects, which result in the formation of edge modes (bound states, localized states). These are also essential in the analysis of finite systems in Section 3.3.
First, we analyse the situation where $E = 0$. Consequently, Eqs. (3.29) and (3.30) take the following form:

$$vB_n + wB_{n-1} = 0, \tag{3.77}$$

$$wA_{n+1} + vA_n = 0. \tag{3.78}$$

The solution of Eqs. (3.77) and (3.78) can be written as:

$$B_n = b\left(-\frac{w}{v}\right)^n, \tag{3.79}$$

$$A_n = a\left(-\frac{v}{w}\right)^n, \tag{3.80}$$

where a and b are constants.
In the case of a semi-infinite waveguide we choose the boundary condition such that $B_0 = 0$, then also $B_n = 0$. In this case, we consider a solution for A_n given by Eq. (3.80).
If $v < w$, then it holds that

$$\lim_{n\to\infty} A_n = 0, \quad n \geq 1. \tag{3.81}$$

From here, we see that there is a localized state located in the left part of the waveguide, where it gradually attenuates.
For the case where $w < v$, as $n \to \infty$, we would arrive at a non-physical conclusion (unbounded solution), hence there is no localized state for the relation $w < v$.

3.3 Finite Structure

We now consider a finite system with a finite Hermitian matrix (derived from Eq. (3.32)). Also for the finite case it is necessary to specify the boundary conditions of such a system, because finite systems (as well as semi-infinite ones) lead to the consideration of boundary effects and consequently to the existence of edge modes.
We terminate the semi-infinite waveguide from Eqs. (3.79) and (3.80), for instance, at the location $x = x^A_{N+1}$, where the boundary condition $A_{N+1} = 0$ holds. For $E = 0$, we can also write the solution to Eq. (3.77) in the following way:

$$B_n = b\left(-\frac{v}{w}\right)^{N-n}, \quad n \leq N, \tag{3.82}$$

while $A_n = 0$. The state is now localized in the right part of the waveguide.
Thus, for a finite waveguide, one can express, for $E = 0$ (more precisely, $E \approx 0$ since it represents the only option to satisfy the finite waveguide conditions), the normalized solution for the aforementioned two boundary conditions as a linear combination:

$$P^b_n = \frac{1}{\sqrt{2}}(A_n \pm B_n) = \sqrt{\frac{1-\left(\frac{v}{w}\right)^2}{2}}\left[\left(-\frac{v}{w}\right)^n \pm \left(-\frac{v}{w}\right)^{N-n}\right], \quad v < w, \tag{3.83}$$

where the constants a and b were determined so that the following relation (normalization condition) holds:

$$\sum_n \left[\left(\frac{A_n}{\sqrt{2}}\right)^2 + \left(\frac{B_n}{\sqrt{2}}\right)^2\right] \approx 1. \tag{3.84}$$

Note that if $n \to \infty$, then Eq. (3.84) is equal to one.
Edge modes are topologically protected (see e.g. [6, 11]) because they persist under continuous deformations of the system until the closure of the band gap occurs.

We now express the matrix $\mathbf{H}_+$ from Eq. (3.55) in a more compact form. For this purpose, we rewrite this matrix in the following form:

$$\mathbf{H}_+ = \begin{pmatrix} 0 & v + we^{-\mathrm{j}q} \\ v + we^{\mathrm{j}q} & 0 \end{pmatrix} = \begin{pmatrix} 0 & v + w\cos(q) - \mathrm{j}w\sin(q) \\ v + w\cos(q) + \mathrm{j}w\sin(q) & 0 \end{pmatrix}. \tag{3.85}$$

Utilizing the Pauli matrices

$$\sigma_x = \begin{pmatrix} 0 & 1 \\ 1 & 0 \end{pmatrix}, \quad \sigma_y = \begin{pmatrix} 0 & -\mathrm{j} \\ \mathrm{j} & 0 \end{pmatrix}, \quad \sigma_z = \begin{pmatrix} 1 & 0 \\ 0 & -1 \end{pmatrix}, \tag{3.86}$$

the compact form can be expressed as follows:

$$\mathbf{H}_+(q) = \boldsymbol{h}(q) \cdot \boldsymbol{\sigma} = \big(h_x(q), h_y(q), h_z(q)\big) \cdot \big(\sigma_x, \sigma_y, \sigma_z\big)^{\mathsf{T}}, \tag{3.87}$$

where

$$\boldsymbol{h}(q) = \big(h_x(q), h_y(q), h_z(q)\big) = \big(v + w\cos(q), w\sin(q), 0\big). \tag{3.88}$$

We introduce a complex function:

$$\hat{h}(q) = h_x(q) + \mathrm{j}h_y(q) = v + we^{\mathrm{j}q} = \left|\hat{h}(q)\right| e^{\mathrm{j}\theta(q)} = |\boldsymbol{h}(q)|\, e^{\mathrm{j}\theta(q)} = \left|v + we^{\mathrm{j}q}\right| e^{\mathrm{j}\theta(q)}, \tag{3.89}$$

where

$$\theta(q) = \arg\left(v + we^{\mathrm{j}q}\right) = \arctan\left(\frac{h_y(q)}{h_x(q)}\right). \tag{3.90}$$

Employing $\hat{h}(q)$, the matrix $\mathbf{H}_+$ can be expressed as:

$$\mathbf{H}_+ = \begin{pmatrix} 0 & \hat{h}^*(q) \\ \hat{h}(q) & 0 \end{pmatrix}. \tag{3.91}$$

Additionally, it holds that

$$\mathbf{H}_- = \begin{pmatrix} 0 & \hat{h}(q) \\ \hat{h}^*(q) & 0 \end{pmatrix}. \tag{3.92}$$

The trajectories (circles) of the terminal point of vector $\boldsymbol{h}(q)$ are depicted in Fig. 3.4. Cases $v > w$ and $v < w$ are not topologically equivalent because it is not possible to transition smoothly from one case to another, as it would require crossing the state $v = w$. We refer to the case $v > w$ as topologically trivial and to the case $v < w$ as topologically non-trivial.

Definition. *Let ζ be a closed piecewise smooth curve, and let a point z_0 not lie on it:*

$$\zeta : [a; b] \to \mathbb{C} \setminus z_0.$$

We then define the winding number (winding index) of ζ around z_0 as:

$$\mathcal{N}(\zeta, z_0) = \frac{1}{2\pi\mathrm{j}} \int_\zeta \frac{\mathrm{d}z}{z - z_0}. \tag{3.93}$$

The winding number $\mathcal{N}(\zeta, z_0)$ is always a non-negative integer and from a geometric perspective, it indicates how many times the curve ζ encircles a point z_0. For a point lying outside the curve, the winding number of the point is always equal to zero.
Expressing the curve ζ in polar coordinates, i.e.,

$$\zeta(q) = z_0 + r(q)e^{\mathrm{j}\theta(q)}, \tag{3.94}$$

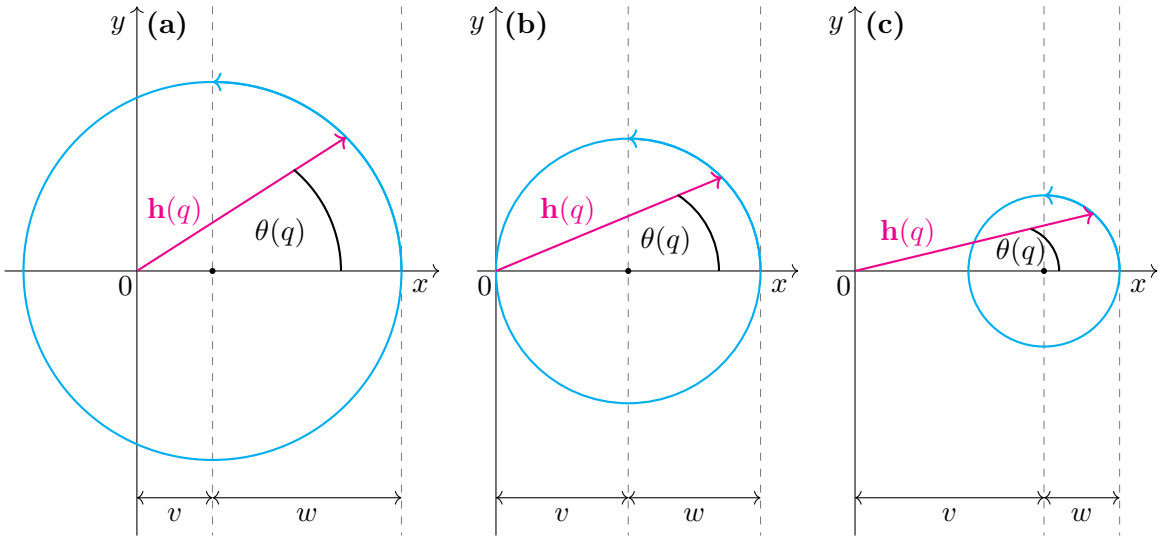

Fig. 3.4: The endpoint trajectory of the vector $\mathbf{h}(q)$ located at the origin. Coordinates for different values of v and w ($q \in [-\pi;\pi]$): **(a)** $v < w$, **(b)** $v = w$, **(c)** $v > w$.

and utilizing the fact that ζ is a closed curve, i.e., $r(a) = r(b)$, based on the definition, we can calculate the winding number $\mathcal{N}(\zeta, z_0)$ on the curve ζ around a point z_0 as:

$$\mathcal{N}(\zeta, z_0) = \frac{1}{2\pi \mathrm{j}} \int_{\zeta} \frac{\mathrm{d}z}{z - z_0} = \frac{1}{2\pi \mathrm{j}} \int_a^b \frac{\zeta'(q)}{\zeta(q) - z_0} \mathrm{d}q = \frac{1}{2\pi \mathrm{j}} \int_a^b \frac{\mathrm{j} r(q)\theta'(q) e^{\mathrm{j}\theta(q)} + r'(q) e^{\mathrm{j}\theta(q)}}{r(q) e^{\mathrm{j}\theta(q)}} \mathrm{d}q = \frac{1}{2\pi \mathrm{j}} \int_a^b \left[\mathrm{j}\theta'(q) + \frac{r'(q)}{r(q)} \right] \mathrm{d}q = \frac{1}{2\pi \mathrm{j}} \int_a^b \ln' \left[\zeta(q) \right] \mathrm{d}q, \quad (3.95)$$

where the prime denotes the first derivative of a function with respect to q. In the considered case (see Fig. 3.4), the point z_0 is located at the origin of coordinates ($z_0 = 0$), $a = -\pi$, $b = \pi$, and $\zeta \equiv \hat{h}(q) = \left| \hat{h}(q) \right| e^{\mathrm{j}q}$, and thus

$$\mathcal{N}\left[\hat{h}(q), 0 \right] = \frac{1}{2\pi \mathrm{j}} \int_{-\pi}^{\pi} \ln' \left[\hat{h}(q) \right] \mathrm{d}q = \begin{cases} 1 & \text{if } v < w, \\ 0 & \text{if } v > w. \end{cases} \quad (3.96)$$

For the case $v < w$, it always holds that $\mathcal{N}\left(\hat{h}, 0\right) = 1$, and for the case $v > w$, it always holds that $\mathcal{N}\left(\hat{h}, 0\right) = 0$, see Fig. 3.4. If we have two distinct winding numbers $\mathcal{N}\left(\hat{h}, 0\right)$ for cases $v < w$ and $v > w$, it implies the existence of a topological transition for $v = w$, i.e., there is a closure of the band gap. Note that the winding number as a criterion for the existence of edge modes has its limits, as shown in Case **(A)** later in this section.

As in Chapter 2, we now focus on the analysis of four specific finite acoustic waveguides. Using the relations derived in this section within the SSH model, we can determine their properties based on boundary conditions.

(A) Finite locally periodic symmetric structure with open ends

We consider an open finite acoustic waveguide containing $2N+1$ elements, thus resulting in $2N$ edges, as illustrated in Fig. 3.5. The waveguide begins and ends with an open element having the cross-section S_B. The number of cells (N) affects the density of states; the larger the value of N, the higher the density of states becomes. Given that the waveguide is open, the Dirichlet boundary conditions are considered at both ends. Radiative losses can be neglected, except when dealing with small cross-sectional areas S_B.

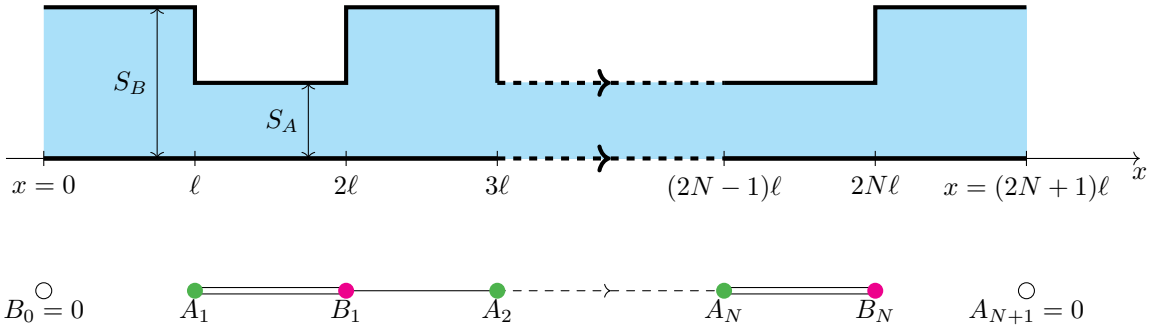

Fig. 3.5: Open boundary conditions and an even number of edges $2N$.

Assuming the boundary conditions, it must hold that

$$B_0 = A_{N+1} = 0. \tag{3.97}$$

For the case under consideration, we now compute the eigenmodes of such a waveguide. Considering specifically the case where $N = 5$, we utilize the boundary conditions expressed by Eq. (3.97), then from Eqs. (3.29) and (3.30), we obtain:

$$\begin{aligned} vB_1 &= EA_1, \\ wA_2 + vA_1 &= EB_1, \\ vB_2 + wB_1 &= EA_2, \\ wA_3 + vA_2 &= EB_2, \\ &\vdots \\ vA_5 &= EB_5. \end{aligned} \tag{3.98}$$

This leads us to the following Hermitian matrix ($2N \times 2N$, that is 10×10 for $N = 5$):

$$\mathbf{H}_{\mathrm{A}} = \begin{pmatrix} 0 & v & 0 & 0 & 0 & 0 & 0 & 0 & 0 & 0 \\ v & 0 & w & 0 & 0 & 0 & 0 & 0 & 0 & 0 \\ 0 & w & 0 & v & 0 & 0 & 0 & 0 & 0 & 0 \\ 0 & 0 & v & 0 & w & 0 & 0 & 0 & 0 & 0 \\ 0 & 0 & 0 & w & 0 & v & 0 & 0 & 0 & 0 \\ 0 & 0 & 0 & 0 & v & 0 & w & 0 & 0 & 0 \\ 0 & 0 & 0 & 0 & 0 & w & 0 & v & 0 & 0 \\ 0 & 0 & 0 & 0 & 0 & 0 & v & 0 & w & 0 \\ 0 & 0 & 0 & 0 & 0 & 0 & 0 & w & 0 & v \\ 0 & 0 & 0 & 0 & 0 & 0 & 0 & 0 & v & 0 \end{pmatrix}, \tag{3.99}$$

which allows us to formulate the eigenvalue problem as follows:

$$\mathbf{H}_{\mathrm{A}} \boldsymbol{X}_{\mathrm{A}} = E \boldsymbol{X}_{\mathrm{A}}, \tag{3.100}$$

where

$$\boldsymbol{X}_{\mathrm{A}} = (A_1, B_1, \ldots, A_5, B_5)^{\intercal}. \tag{3.101}$$

The eigenvalues $E_i = \cos(k_i \ell)$, where k_i are the eigen-wave numbers and $i = 1, \ldots, 2N$, are found as the roots of the following polynomial equation:

$$\det(\mathbf{H}_{\mathrm{A}} - E\mathbf{I}) = 0. \tag{3.102}$$

The frequency width of the band gap is calculated for $q = -\pi$ or $q = \pi$ (the first Brillouin zone) from Eq. (3.60), we thus obtain:

$$\cos(k\ell) = \pm(v - w). \tag{3.103}$$

Given this, we calculate the lower frequency f_{lb} (lower boundary) and the upper frequency f_{ub} (upper boundary) of the band gap as:

$$f_{\mathrm{lb}} = \frac{c_0 \arccos[-(v - w)]}{2\pi\ell}, \tag{3.104}$$

$$f_{\mathrm{ub}} = \frac{c_0 \arccos[+(v - w)]}{2\pi\ell}. \tag{3.105}$$

For the width of the band gap, we can write as follows:

$$\Delta_f = f_{\mathrm{ub}} - f_{\mathrm{lb}}. \tag{3.106}$$

For $v = w$, it holds that $f_{\mathrm{lb}} = f_{\mathrm{ub}}$, thus $\Delta_f = 0$ (resulting in the closure of the band gap). Using the obtained eigenvalues $E_i = \cos(k_i \ell)$, the eigenfrequencies f_i can also be determined as:

$$f_i = \frac{c_0 \arccos(E_i)}{2\pi\ell}. \tag{3.107}$$

We assume that $E = E_+ > 0$. We determine the eigenmodes using Eq. (3.76), which we now restate:

$$\begin{pmatrix} A_n \\ B_n \end{pmatrix} = \alpha e^{\mathrm{j}nq} \begin{pmatrix} 1 \\ e^{\mathrm{j}\theta(q)} \end{pmatrix} + \beta e^{-\mathrm{j}nq} \begin{pmatrix} 1 \\ e^{-\mathrm{j}\theta(q)} \end{pmatrix}, \tag{3.108}$$

where α and β are complex integration constants that need to be determined. Additionally, we recall that $\theta(q) = \arg\left(v + we^{\mathrm{j}q}\right)$. Furthermore, it is also possible to express Eq. (3.108) using the eigenvectors obtained through the gauge transformation:

$$\begin{pmatrix} A_n \\ B_n \end{pmatrix} = \alpha e^{\mathrm{j}nq} \begin{pmatrix} e^{-\mathrm{j}\theta(q)} \\ 1 \end{pmatrix} + \beta e^{-\mathrm{j}nq} \begin{pmatrix} e^{\mathrm{j}\theta(q)} \\ 1 \end{pmatrix}. \tag{3.109}$$

In order to satisfy the boundary condition such that $B_0 = 0$, Eq. (3.109) implies that $\alpha = -\beta$. Following equations can be written:

$$A_n = \tilde{\alpha} \frac{e^{\mathrm{j}[nq-\theta(q)]} - e^{-\mathrm{j}[nq-\theta(q)]}}{2\mathrm{j}} = \tilde{\alpha} \sin\left[nq - \theta(q)\right], \tag{3.110}$$

$$B_n = \tilde{\alpha} \frac{e^{\mathrm{j}nq} - e^{-\mathrm{j}nq}}{2\mathrm{j}} = \tilde{\alpha} \sin(nq), \tag{3.111}$$

where $\tilde{\alpha} = 2\mathrm{j}\alpha$.
In order to satisfy the boundary condition such that $A_{N+1} \equiv A_6 = 0$, we use Eq. (3.110) and obtain as follows:

$$\sin\left[(N+1)q - \theta(q)\right] = 0 \quad \Longrightarrow \quad \sin\left[6q - \arg\left(v + we^{\mathrm{j}q}\right)\right] = 0. \tag{3.112}$$

This equation is satisfied only for certain values of q from the interval $(-\pi; \pi)$. Since it is an odd function, it is sufficient to calculate the roots from the interval $(0; \pi)$, while the roots in the interval $(-\pi; 0)$ are negative. The point $q = 0$ is always a root of the equation. It is also important to note that the roots of this equation depend on the coupling coefficients v and w. Furthermore, this method can find only the eigenfrequencies for bulk modes, whereas by solving Eq. (3.102), we also obtain the eigenfrequencies for edge modes.
For Eq. (3.112) to be satisfied, it must hold that

$$(N+1)q - \theta(q) = m\pi, \tag{3.113}$$

where m is an integer. Graphically, the solution of Eq. (3.113) for $q \in (0; \pi)$ can be found by looking for the intersections of the function $\theta(q)$ with the following function:

$$g_m(q) = (N+1)q - m\pi. \tag{3.114}$$

This is shown in Fig. 3.6 for $N = 5$. From this figure, it is evident that the winding number determines the existence of bulk (non-localized) modes, and thus the existence of edge (localized) modes.
It can also be seen that for $v > w$, $\theta(\pi) = 0$ and Eq. (3.113) has N solutions, whereas for $v < w$, $\theta(\pi) = \pi$ and this equation has N or $N-1$ solutions depending on the ratio of v/w.

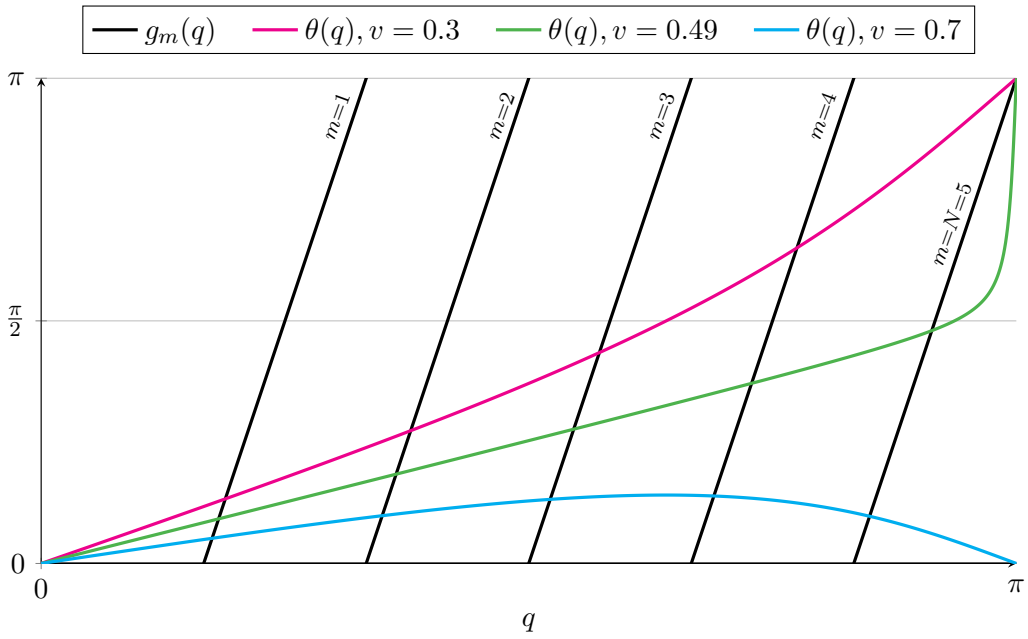

Fig. 3.6: Determination of the number of bulk modes depending on the value of v.

By comparing the slope of the curves $\theta(q)$ and $g_N(q)$, we can determine the number of bulk modes with respect to the critical ratio $r_\mathrm{c} = (v/w)_\mathrm{c}$, which we formulate using Eq. (3.90) as follows:

$$\left(\frac{\mathrm{d}\theta(q)}{\mathrm{d}q}\right)_{q=\pi} = \left[\frac{\mathrm{d}}{\mathrm{d}q}\arctan\left(\frac{h_y}{h_x}\right)\right]_{q=\pi} = \left[\frac{\mathrm{d}}{\mathrm{d}q}\arctan\left(\frac{\sin(q)/r_\mathrm{c}}{1+\cos(q)/r_\mathrm{c}}\right)\right]_{q=\pi} = \frac{1}{1-r_\mathrm{c}}. \quad (3.115)$$

This result must be equal to the slope of the line $g_N(q)$, i.e.,

$$\frac{1}{1-r_\mathrm{c}} = N+1. \quad (3.116)$$

From this, it holds that

$$r_\mathrm{c} = \left(\frac{v}{w}\right)_\mathrm{c} = \frac{N}{N+1} = 1 - \frac{1}{N+1}. \quad (3.117)$$

From Fig. 3.6, we see that for $r_\mathrm{c} < v/w < 1$, there exists one more bulk mode for $q \in (0;\pi)$ than in the case $v/w < r_\mathrm{c}$. If we also consider negative values of q, then we must multiply the number of bulk modes by a factor of two, thus the total number of bulk modes M_t is:

$$M_\mathrm{t} = 2N, \quad \text{for} \quad \frac{v}{w} > r_\mathrm{c}, \quad (3.118)$$

and

$$M_\mathrm{t} = 2(N-1), \quad \text{for} \quad \frac{v}{w} < r_\mathrm{c}. \quad (3.119)$$

From this, we can conclude that for N finite, there exist coupling coefficients v and w such that for $r_\mathrm{c} < v/w < 1$ there are no edge modes, even though the winding number is equal to 1 (in this case, two bulk modes replace two edge modes). With increasing N, the interval $r_\mathrm{c} < v/w < 1$, for which no edge modes exist under the condition $v < w$, decreases.

Specifically for $N = 5$, the critical ratio $r_\mathrm{c} = (v/w)_\mathrm{c}$ formulated in Eq. (3.117) is given as follows:

$$r_\mathrm{c} = \frac{5}{6} = 0.8\overline{3}. \tag{3.120}$$

Since the coupling coefficient $v = 0.3$, it holds that $v/w = \frac{3}{7}$ and therefore $v/w < r_\mathrm{c} < 1$. From Fig. 3.6, we see that for $v = 0.3$, there exists no more bulk mode for $q \in (0; \pi)$. We thus obtain $M_\mathrm{t} = 2(N-1) = 8$ as stated in Eq. (3.119).
Considering $N = 5$ and $v = 0.49$, we find that $r_\mathrm{c} < v/w = \frac{49}{51} \doteq 0.96 < 1$, leading us to the other case where $M_\mathrm{t} = 2N = 10$ expressed in Eq. (3.118). This results in all eigenmodes lying outside of the band gap, which in turn yields two additional bulk modes and no edge modes.

(B) Finite locally periodic symmetric structure with closed ends

We now assume the same finite locally periodic structure as in Case **(A)**. This time, it is terminated on both ends with a perfectly rigid wall, see Fig. 3.7. This results in the acoustic velocity being zero at the location of the perfectly rigid wall, or as derived from the Euler's equation, $P'\left(x_0^{B^+}\right)=0$ and $P'\left(x_{N+1}^{A^-}\right)=0$ (the Neumann boundary conditions).

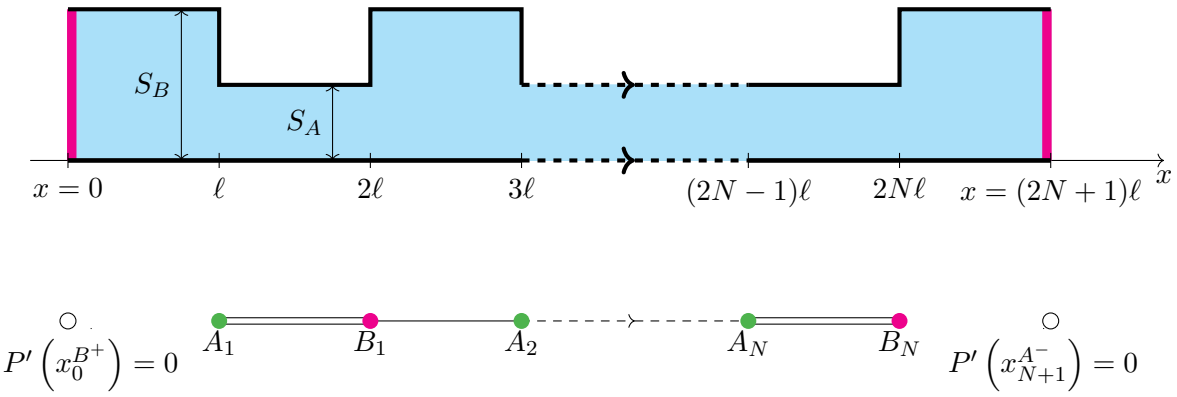

Fig. 3.7: Closed boundary conditions and an even number of edges $2N$.

For an element with the cross-sectional area S_B located in the interval $x\in\left(x_{n-1}^B;x_n^A\right)$, we can express the solution of the Helmholtz equation (2.5) as:

$$P(x)=C_1\sin\left[k\left(x-x_n^A\right)\right]+C_2\cos\left[k\left(x-x_n^A\right)\right], \tag{3.121}$$

where C_1 and C_2 are integration constants that we need to determine.
The derivative of this solution with respect to the variable x is obtained as:

$$\frac{\mathrm{d}P\left(x\right)}{\mathrm{d}x}\equiv P'\left(x\right)=C_1k\cos\left[k\left(x-x_n^A\right)\right]-C_2k\sin\left[k\left(x-x_n^A\right)\right]. \tag{3.122}$$

The integration constant C_2 is determined from Eq. (3.121) as follows:

$$P\left(x_n^A\right)=C_2, \tag{3.123}$$

and the integration constant C_1 is determined from Eq. (3.122):

$$P'\left(x_n^{A^-}\right)=C_1k\quad\Longrightarrow\quad C_1=\frac{P'\left(x_n^{A^-}\right)}{k}. \tag{3.124}$$

Substituting for the integration constants C_1 and C_2 in Eq. (3.121), we obtain:

$$P(x)=\frac{P'\left(x_n^{A^-}\right)}{k}\sin\left[k\left(x-x_n^A\right)\right]+P\left(x_n^A\right)\cos\left[k\left(x-x_n^A\right)\right]. \tag{3.125}$$

Solving Eq. (3.125) at $x = x_{n-1}^{B}$, we thus obtain as follows:

$$P\left(x_{n-1}^{B}\right) = \frac{P'\left(x_{n}^{A^-}\right)}{k}\sin\left[k\left(x_{n-1}^{B} - x_{n}^{A}\right)\right] + P\left(x_{n}^{A}\right)\cos\left[k\left(x_{n-1}^{B} - x_{n}^{A}\right)\right]. \tag{3.126}$$

Since $x_{n-1}^{B} - x_{n}^{A} = -\ell$, we rewrite Eq. (3.126) in the following form:

$$P\left(x_{n-1}^{B}\right) = \frac{P'\left(x_{n}^{A^-}\right)}{k}\sin\left(-k\ell\right) + P\left(x_{n}^{A}\right)\cos\left(-k\ell\right). \tag{3.127}$$

Because the sine function is an odd function and the cosine function is an even function, Eq. (3.127) can be rewritten in its final form as:

$$\boxed{P\left(x_{n-1}^{B}\right) = -\frac{P'\left(x_{n}^{A^-}\right)}{k}\sin\left(k\ell\right) + P\left(x_{n}^{A}\right)\cos\left(k\ell\right).} \tag{3.128}$$

In a similar manner, we extend the procedure to the subsequent element concerning the cross-sectional area S_B where $x \in \left(x_{n}^{B}; x_{n+1}^{A}\right)$:

$$P(x) = C_3\sin\left[k\left(x - x_{n}^{B}\right)\right] + C_4\cos\left[k\left(x - x_{n}^{B}\right)\right], \tag{3.129}$$

where C_3 and C_4 are integration constants.
Taking the derivative of Eq. (3.129) with respect to the variable x, we obtain:

$$P'(x) = C_3 k\cos\left[k\left(x - x_{n}^{B}\right)\right] - C_4 k\sin\left[k\left(x - x_{n}^{B}\right)\right]. \tag{3.130}$$

The integration constant C_4 is determined from Eq. (3.129):

$$P\left(x_{n}^{B}\right) = C_4, \tag{3.131}$$

and the integration constant C_3 is determined from Eq. (3.130) as follows:

$$P'\left(x_{n}^{B^+}\right) = C_3 k \quad \Longrightarrow \quad C_3 = \frac{P'\left(x_{n}^{B^+}\right)}{k}. \tag{3.132}$$

Substituting for C_3 and C_4 in Eq. (3.129), we obtain the solution for the corresponding element:

$$P(x) = \frac{P'\left(x_{n}^{B^+}\right)}{k}\sin\left[k\left(x - x_{n}^{B}\right)\right] + P\left(x_{n}^{B}\right)\cos\left[k\left(x - x_{n}^{B}\right)\right]. \tag{3.133}$$

Solving Eq. (3.133) at $x = x_{n+1}^{A}$, we obtain as follows:

$$P\left(x_{n+1}^{A}\right) = \frac{P'\left(x_{n}^{B^+}\right)}{k}\sin\left[k\left(x_{n+1}^{A} - x_{n}^{B}\right)\right] + P\left(x_{n}^{A}\right)\cos\left[k\left(x_{n+1}^{A} - x_{n}^{B}\right)\right]. \tag{3.134}$$

Since $x_{n+1}^{A} - x_{n}^{B} = \ell$, we rewrite Eq. (3.134) in the following form:

$$\boxed{P(x_{n+1}^{A}) = \frac{P'(x_{n}^{B^+})}{k}\sin(k\ell) + P(x_{n}^{B})\cos(k\ell).} \tag{3.135}$$

Based on Eq. (3.135), we can write that

$$A_1 = \cos(k\ell)B_0 \equiv E(k)B_0, \tag{3.136}$$

and based on Eq. (3.128), we get that

$$B_N = \cos(k\ell)A_{N+1} \equiv E(k)A_{N+1}. \tag{3.137}$$

Using Eqs. (3.136) and (3.137) and the SSH model expressed by Eqs. (3.29) and (3.30), we can write for $N = 5$:

$$\begin{aligned} A_1 &= EB_0, \\ wB_0 + vB_1 &= EA_1, \\ wA_2 + vA_1 &= EB_1, \\ vB_2 + wB_1 &= EA_2, \\ vA_2 + wA_3 &= EB_2, \\ &\vdots \\ vA_5 + wA_6 &= EB_5, \\ B_5 &= EA_6. \end{aligned} \tag{3.138}$$

This leads us to the following matrix ($(2N + 2) \times (2N + 2)$, that is 12×12 for $N = 5$):

$$\mathbf{H}_{\mathrm{B}} = \begin{pmatrix} 0 & 1 & 0 & 0 & 0 & 0 & 0 & 0 & 0 & 0 & 0 & 0 \\ w & 0 & v & 0 & 0 & 0 & 0 & 0 & 0 & 0 & 0 & 0 \\ 0 & v & 0 & w & 0 & 0 & 0 & 0 & 0 & 0 & 0 & 0 \\ 0 & 0 & w & 0 & v & 0 & 0 & 0 & 0 & 0 & 0 & 0 \\ 0 & 0 & 0 & v & 0 & w & 0 & 0 & 0 & 0 & 0 & 0 \\ 0 & 0 & 0 & 0 & w & 0 & v & 0 & 0 & 0 & 0 & 0 \\ 0 & 0 & 0 & 0 & 0 & v & 0 & w & 0 & 0 & 0 & 0 \\ 0 & 0 & 0 & 0 & 0 & 0 & w & 0 & v & 0 & 0 & 0 \\ 0 & 0 & 0 & 0 & 0 & 0 & 0 & v & 0 & w & 0 & 0 \\ 0 & 0 & 0 & 0 & 0 & 0 & 0 & 0 & w & 0 & v & 0 \\ 0 & 0 & 0 & 0 & 0 & 0 & 0 & 0 & 0 & v & 0 & w \\ 0 & 0 & 0 & 0 & 0 & 0 & 0 & 0 & 0 & 0 & 1 & 0 \end{pmatrix}. \tag{3.139}$$

Given that matrix $\mathbf{H}_{\mathrm{B}}$ is not symmetric ($\mathbf{H}_{\mathrm{B}} \neq \mathbf{H}_{\mathrm{B}}^{\intercal}$), this case does not constitute a Hermitian matrix. The eigenvalue problem is then formulated as follows:

$$\mathbf{H}_{\mathrm{B}}\boldsymbol{X}_{\mathrm{B}} = E\boldsymbol{X}_{\mathrm{B}}, \tag{3.140}$$

where

$$\boldsymbol{X}_{\mathrm{B}} = (B_0, A_1, B_1, \ldots, A_5, B_5, A_6)^{\intercal}. \tag{3.141}$$

The eigenvalues $E_i = \cos(k_i\ell)$ (there is a total of $2N+2$) are found as roots of the following polynomial equation:

$$\det(\mathbf{H}_{\mathrm{B}} - E\mathbf{I}) = 0. \tag{3.142}$$

Then the eigenmodes are calculated according to Eq. (3.107).
Also for this case, we can find the eigenmodes using the approach that in Case **(A)** is based on Eq. (3.109), but now we consider the Neumann boundary conditions (more is solved in this way for the antisymmetric closed structure later in this section in Case **(D)**). It turns out that for this finite locally periodic structure with closed ends, the determination of the eigenmodes is analogous to Case **(A)**, but with a substitution of $v \leftrightarrow w$. This is evident from the results presented in Chapter 4, which are consistent with the TMM approach (see e.g. Figs. 4.1**(A)** and **(B)**).

(C) Finite locally periodic antisymmetric structure with open ends
Next, we consider an open finite acoustic waveguide, containing $2N$ elements and thus $2N-1$ edges, see Fig. 3.8. In contrast to the previous type discussed in Cases **(A)** and **(B)**, it starts with an open element of the cross-section S_B and ends with an open element of S_A. Since the waveguide is open, we consider the Dirichlet boundary conditions at both ends (radiative losses can be neglected unless we consider small cross-sectional areas S_B).

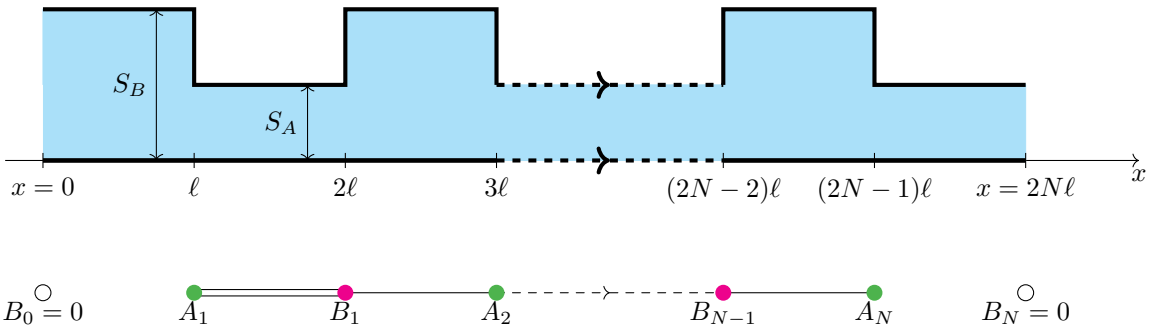

Fig. 3.8: Open boundary conditions and an odd number of edges $2N-1$.

Assuming the aforementioned boundary conditions, then it must hold that

$$B_0 = B_N = 0. \tag{3.143}$$

For the case under consideration, we compute the eigenmodes of such a waveguide. Considering specifically the case where $N = 5$, we utilize the conditions expressed in Eq. (3.143). From Eqs. (3.29) and (3.30), we then obtain:

$$\begin{aligned} vB_1 &= EA_1, \\ wA_2 + vA_1 &= EB_1, \\ vB_2 + wB_1 &= EA_2, \\ wA_3 + vA_2 &= EB_2, \\ &\vdots \\ wB_4 &= EA_5. \end{aligned} \tag{3.144}$$

This leads us to the following Hermitian matrix ($(2N-1)\times(2N-1)$, that is 9×9 for

$N = 5$):

$$\mathbf{H}_{\mathrm{C}} = \begin{pmatrix} 0 & v & 0 & 0 & 0 & 0 & 0 & 0 & 0 \\ v & 0 & w & 0 & 0 & 0 & 0 & 0 & 0 \\ 0 & w & 0 & v & 0 & 0 & 0 & 0 & 0 \\ 0 & 0 & v & 0 & w & 0 & 0 & 0 & 0 \\ 0 & 0 & 0 & w & 0 & v & 0 & 0 & 0 \\ 0 & 0 & 0 & 0 & v & 0 & w & 0 & 0 \\ 0 & 0 & 0 & 0 & 0 & w & 0 & v & 0 \\ 0 & 0 & 0 & 0 & 0 & 0 & v & 0 & w \\ 0 & 0 & 0 & 0 & 0 & 0 & 0 & w & 0 \end{pmatrix}, \tag{3.145}$$

which allows us to formulate the eigenvalue problem as follows:

$$\mathbf{H}_{\mathrm{C}}\boldsymbol{X}_{\mathrm{C}} = E\boldsymbol{X}_{\mathrm{C}}, \tag{3.146}$$

where

$$\boldsymbol{X}_{\mathrm{C}} = (A_1, B_1, \ldots, A_5)^{\intercal}. \tag{3.147}$$

The eigenvalues $E_i = \cos(k_i \ell)$ $(i = 1, \ldots, 2N-1)$ are found as the roots of the following polynomial equation:

$$\det(\mathbf{H}_{\mathrm{C}} - E\mathbf{I}) = 0. \tag{3.148}$$

We assume that $E = E_+ > 0$. We determine the eigenmodes analogously to Case **(A)** using Eqs. (3.108) and (3.109).
In order to satisfy the boundary condition such that $B_0 = 0$, Eq. (3.109) implies that $\alpha = -\beta$. From Eq. (3.109), we thus obtain Eqs. (3.110) and (3.111).
In order to satisfy the boundary condition such that $B_N \equiv B_5 = 0$, from Eq. (3.111), we then obtain the following equation:

$$\sin(Nq) = 0 \quad \Longrightarrow \quad \sin(5q) = 0. \tag{3.149}$$

This equation is satisfied only for certain values of q from the interval $(-\pi; \pi)$. The point $q = 0$ is always a root of the equation. In this case, the roots do not depend on the coupling coefficients v or w. Again, this method can find only the eigenfrequencies for bulk modes, whereas by solving Eq. (3.148), we also obtain the eigenfrequencies for edge modes.
For Eq. (3.149) to be satisfied, it must hold that

$$Nq = m\pi, \tag{3.150}$$

where m is an integer.

(D) Finite locally periodic antisymmetric structure with closed ends
We now assume the acoustic waveguide (finite locally periodic structure) as in Case **(C)**, but on both ends there is a perfectly rigid wall terminating the structure (see Fig. 3.9), resulting in the Neumann boundary conditions: $P'\left(x_0^{B^+}\right)=0$ and $P'\left(x_N^{B^-}\right)=0$.

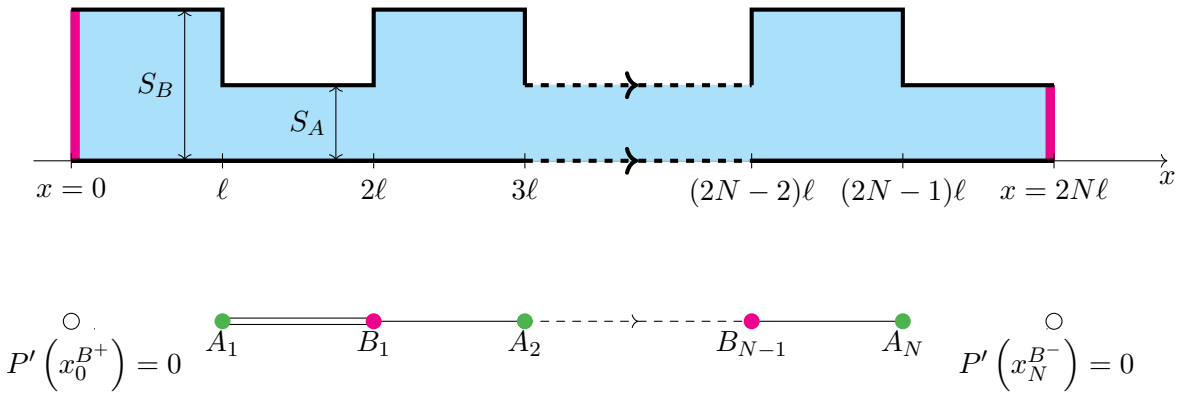

Fig. 3.9: Closed boundary conditions and an odd number of edges $2N-1$.

For an element with the cross-sectional area S_A lying in the interval of $x\in\left(x_n^A;x_n^B\right)$ (as depicted in Fig. 3.2), we can express the solution of the Helmholtz equation (2.5) as:

$$P(x)=C_5\sin\left[k\left(x-x_n^B\right)\right]+C_6\cos\left[k\left(x-x_n^B\right)\right], \tag{3.151}$$

where C_5 and C_6 are integration constants.
Taking the derivative of Eq. (3.151) with respect to the variable x, we obtain:

$$P'(x)=C_5k\cos\left[k\left(x-x_n^B\right)\right]-C_6k\sin\left[k\left(x-x_n^B\right)\right]. \tag{3.152}$$

The integration constant C_6 is determined from Eq. (3.151) as follows:

$$P\left(x_n^B\right)=C_6, \tag{3.153}$$

and C_5 is determined from Eq. (3.152):

$$P'\left(x_n^{B^-}\right)=C_5k \quad\Longrightarrow\quad C_5=\frac{P'\left(x_n^{B^-}\right)}{k}. \tag{3.154}$$

Substituting for C_5 and C_6 in Eq. (3.151), we obtain:

$$P(x)=\frac{P'\left(x_n^{B^-}\right)}{k}\sin\left[k\left(x-x_n^B\right)\right]+P\left(x_n^B\right)\cos\left[k\left(x-x_n^B\right)\right]. \tag{3.155}$$

We note that solutions (3.155) and (3.133) are identical at $x=x_n^B$.
Solving Eq. (3.155) at $x=x_n^A$, we thus obtain as follows:

$$P\left(x_n^A\right)=\frac{P'\left(x_n^{B^-}\right)}{k}\sin\left[k\left(x_n^A-x_n^B\right)\right]+P\left(x_n^A\right)\cos\left[k\left(x_n^A-x_n^B\right)\right]. \tag{3.156}$$

Since $x_n^A - x_n^B = -\ell$, we rewrite Eq. (3.156) in the following form:

$$\boxed{P\left(x_n^A\right) = -\frac{P'\left(x_n^{B^-}\right)}{k}\sin(k\ell) + P\left(x_n^B\right)\cos(k\ell).} \tag{3.157}$$

Based on Eq. (3.135), we can write that

$$A_1 = \cos(k\ell)B_0 \equiv E(k)B_0, \tag{3.158}$$

and based on Eq. (3.157), we get that

$$A_N = \cos(k\ell)B_N \equiv E(k)B_N. \tag{3.159}$$

Using Eqs. (3.158) and (3.159) and the SSH model expressed by Eqs. (3.29) and (3.30), we can write for $N = 5$:

$$\begin{aligned}
A_1 &= EB_0, \\
wB_0 + vB_1 &= EA_1, \\
wA_2 + vA_1 &= EB_1, \\
vB_2 + wB_1 &= EA_2, \\
vA_2 + wA_3 &= EB_2, \\
&\vdots \\
wB_4 + vB_5 &= EA_5, \\
A_5 &= EB_5.
\end{aligned} \tag{3.160}$$

This leads us to the following matrix ($(2N+1)\times(2N+1)$, that is 11×11 for $N=5$):

$$\mathbf{H}_{\mathrm{D}} = \begin{pmatrix}
0 & 1 & 0 & 0 & 0 & 0 & 0 & 0 & 0 & 0 & 0 \\
w & 0 & v & 0 & 0 & 0 & 0 & 0 & 0 & 0 & 0 \\
0 & v & 0 & w & 0 & 0 & 0 & 0 & 0 & 0 & 0 \\
0 & 0 & w & 0 & v & 0 & 0 & 0 & 0 & 0 & 0 \\
0 & 0 & 0 & v & 0 & w & 0 & 0 & 0 & 0 & 0 \\
0 & 0 & 0 & 0 & w & 0 & v & 0 & 0 & 0 & 0 \\
0 & 0 & 0 & 0 & 0 & v & 0 & w & 0 & 0 & 0 \\
0 & 0 & 0 & 0 & 0 & 0 & w & 0 & v & 0 & 0 \\
0 & 0 & 0 & 0 & 0 & 0 & 0 & v & 0 & w & 0 \\
0 & 0 & 0 & 0 & 0 & 0 & 0 & 0 & w & 0 & v \\
0 & 0 & 0 & 0 & 0 & 0 & 0 & 0 & 0 & 1 & 0
\end{pmatrix}. \tag{3.161}$$

Given that matrix $\mathbf{H}_{\mathrm{D}}$ is not symmetric ($\mathbf{H}_{\mathrm{D}} \neq \mathbf{H}_{\mathrm{D}}^{\intercal}$), this case does not constitute a Hermitian matrix. The eigenvalue problem can again be written as:

$$\mathbf{H}_{\mathrm{D}}\boldsymbol{X}_{\mathrm{D}} = E\boldsymbol{X}_{\mathrm{D}}, \tag{3.162}$$

where

$$\boldsymbol{X}_{\mathrm{D}} = (B_0, A_1, B_1, \ldots, A_5, B_5)^{\intercal}. \tag{3.163}$$

The eigenvalues $E_i = \cos(k_i \ell)$ (there is a total of $2N+1$) are found as roots of the following polynomial equation:

$$\det(\mathbf{H}_\mathrm{D} - E\mathbf{I}) = 0. \tag{3.164}$$

Then the eigenfrequencies (including edge modes) are calculated according to Eq. (3.107). One of the eigenvalues of this structure is equal to zero, i.e., $\cos(k\ell) = 0$. From here we get the eigenfrequency f_e corresponding to the edge mode:

$$f_\mathrm{e} = \frac{c_0 \arccos(0)}{2\pi\ell} = \frac{c_0}{4\ell}, \tag{3.165}$$

which is equal to the first resonance frequency of a quarter-wave resonator of length ℓ.
It holds that $E = 0$ for f_e, so the solutions of Eqs. (3.77) and (3.78) can be written (see Eq. (3.80)) as:

$$\begin{pmatrix} A_n \\ B_n \end{pmatrix} = b \begin{pmatrix} 0 \\ 1 \end{pmatrix} \left(-\frac{w}{v}\right)^n, \quad w > v, \quad n = 0, 1, \ldots, N, \tag{3.166}$$

where b is a normalization constant. Since $A_0 = 0$, then $A_n = 0$ as well.
The eigenfrequencies of the bulk modes can also be obtained from Eq. (3.109), if we consider that at the point $x = x_0^B$ the acoustic pressure is non-zero ($B_0 \neq 0$), in contrast to the acoustic velocity, and represents an antinode at this point. Then Eq. (3.109) for $n = 0$ shows that

$$\alpha + \beta = B_0 \quad \Longrightarrow \quad \beta = B_0 - \alpha. \tag{3.167}$$

Similarly, for $x = x_N^B$, where the acoustic velocity is also zero, the acoustic pressure must be $B_N \neq 0$ and is represented by an antinode. Thus, from Eq. (3.109), given Eq. (3.167), we get for $n = N$ that

$$B_N = \alpha e^{\mathrm{j}Nq} + (B_0 - \alpha) e^{-\mathrm{j}Nq}. \tag{3.168}$$

We modify this equation into the following form:

$$B_N = \tilde{\alpha} \sin(Nq) + B_0 \cos(Nq) - \mathrm{j} B_0 \sin(Nq), \tag{3.169}$$

where $\tilde{\alpha} = \mathrm{j}2\alpha$.
Since the acoustic pressures B_0 and B_N represent real values, Eq. (3.169) can be satisfied if the following condition is satisfied:

$$\sin(Nq) = 0 \quad \text{or} \quad \cos(Nq) = \pm 1. \tag{3.170}$$

By substituting this condition into Eq. (3.169), we obtain:

$$B_N = B_0 \cos(Nq). \tag{3.171}$$

Considering the condition (3.170), it follows that $B_N = \pm B_0$ and bulk modes are either symmetric or antisymmetric. The value of N, which refers to the number of edges in the waveguide, i.e., $2N+1$, and the value of the dimensionless Bloch wave number $q \in (-\pi; \pi)$ decide which sign to use. That means, it must hold that

$$Nq = m\pi, \tag{3.172}$$

where m is an integer.
The condition that the acoustic pressures B_0 and B_N must be real can also be satisfied when

$$\mathrm{j}B_0 = \tilde{\alpha} = \mathrm{j}2\alpha \quad \Longrightarrow \quad B_0 = 2\alpha, \tag{3.173}$$

see Eq. (3.169). From this result, and considering Eq. (3.167), it follows that in this case $\alpha = \beta$, where these are real values. If we substitute $\mathrm{j}B_0 = \tilde{\alpha}$ into Eq. (3.169), then we obtain as follows:

$$B_N = 2\alpha \cos(Nq) = B_0 \cos(Nq). \tag{3.174}$$

We note that the results expressed in Eqs. (3.171) and (3.174) are identical.
For B_N to represent an antinode, it must hold that $\cos(Nq) = \pm 1$, so we arrive at the same result as when applying the condition (3.170).

Chapter 4

Calculation of Eigenmodes of Specific Acoustic Waveguides

In Chapters 2 and 3, we delved into the analysis of resonant and transmission properties of locally periodic binary structures, employing the Transfer Matrix Method (TMM) and the one-dimensional Su-Schrieffer-Heeger (SSH) model, respectively. We illustrated these methods through specific acoustic waveguides, showcasing functional dependencies and relationships. While both the TMM and the SSH model approaches helped us express the eigenmodes, they represent fundamentally different analytical methods. In this chapter, we focus on the calculation of the numerical values of the bulk and edge modes. We use the TMM as a reference to validate the frequency property calculations derived from the SSH model, offering a deeper comparative analysis and insights into their respective utilities and limitations (more details in Chapter 5).

We categorize our calculations into four distinct special cases, similar to the approach in the previous text (as demonstrated in Fig. 2.6). Each case represents a unique structure, defined by its specific boundary conditions. Obtained relationships enable us to determine the eigenfrequencies, their number, and the characteristics of the band gaps. For illustration, we choose the previously used acoustic waveguide parameters in all four cases, see Tab. 4.1. All numerical values for the calculated eigenfrequencies presented in the tables below are rounded to two decimal places. However, more accurate values can be obtained by using the scripts attached to this thesis. A list of these is provided in Appendix A.
Using Eqs. (3.104) and (3.105), we calculate the frequency boundaries of the band gap, from which we can easily obtain its width by substituting the values of the considered structure into Eq. (3.106). The results are presented in Tab. 4.2. The eigenmodes falling within the band gap frequency interval are then recognised as edge modes and are marked as such in the tables of results.

Parameter	Symbol	Value
Number of cells	N	5
Coupling coefficient	v	0.3
Coupling coefficient	w	0.7
Element length	ℓ	0.05 m
Speed of acoustic wave propagation	c_0	343 ms^{-1}
Frequency range	f	$[0; 3{,}430]$ Hz

Tab. 4.1: Parameters for the analysed locally periodic structures.

Lower band gap frequency f_{lb}
f_{lb} = 1,265.70 Hz
Upper band gap frequency f_{ub}
f_{ub} = 2,164.30 Hz
Band gap width Δ_f
Δ_f = 898.59 Hz

Tab. 4.2: Calculation of the band gap frequency properties for $v = 0.3$.

(A) Finite locally periodic symmetric structure with open ends
We start with the case of the symmetric structure shown in Fig. 2.6**(A)**. Using Eq. (3.107), eigenmodes of the considered waveguide can be calculated. The values found correspond to the roots of the function $\nu(f)$ as expressed in Eq. (2.70) using the TMM. We note that in this case, f_{11} = 3,430 Hz (as shown in Fig. 2.7**(A)**) cannot be obtained using the SSH approach introduced in Chapter 3.

(B) Finite locally periodic symmetric structure with closed ends
Considering the symmetric structure with closed ends as shown in Fig. 2.6**(B)**, we use Eq. (3.107) again to calculate the eigenmodes. Also in this case, the values found correspond to the result obtained from the TMM, e.g. roots of the function $\varphi(f)$ from Eq. (2.79). We note that in this case, f_{12}^{B} = 3,430 Hz and also $f_1^{\text{B}} = 0$ Hz are both obtained using the SSH approach introduced in Chapter 3.

Eigenmode frequency f_i^{A}	Mode type
f_1^{A} = 296.14 Hz	Bulk
f_2^{A} = 589.28 Hz	Bulk
f_3^{A} = 873.61 Hz	Bulk
f_4^{A} = 1,130.11 Hz	Bulk
f_5^{A} = 1,705.97 Hz	Edge
f_6^{A} = 1,724.03 Hz	Edge
f_7^{A} = 2,299.89 Hz	Bulk
f_8^{A} = 2,556.39 Hz	Bulk
f_9^{A} = 2,840.72 Hz	Bulk
f_{10}^{A} = 3,133.86 Hz	Bulk

Tab. 4.3: The eigenmodes for Case **(A)**.

Eigenmode frequency f_i^{B}	Mode type
f_1^{B} = 0.00 Hz	Bulk
f_2^{B} = 275.00 Hz	Bulk
f_3^{B} = 544.82 Hz	Bulk
f_4^{B} = 801.75 Hz	Bulk
f_5^{B} = 1,030.60 Hz	Bulk
f_6^{B} = 1,200.58 Hz	Bulk
f_7^{B} = 2,229.42 Hz	Bulk
f_8^{B} = 2,399.40 Hz	Bulk
f_9^{B} = 2,628.25 Hz	Bulk
f_{10}^{B} = 2,885.18 Hz	Bulk
f_{11}^{B} = 3,155.02 Hz	Bulk
f_{12}^{B} = 3,430.00 Hz	Bulk

Tab. 4.4: The eigenmodes for Case **(B)**.

(C) Finite locally periodic antisymmetric structure with open ends
For Case **(C)**, the waveguide is shown in Fig. 2.6**(C)**. The eigenmodes are calculated using Eq. (3.148) and Eq. (3.107), and presented in Tab. 4.5. Compared to the results calculated as the roots of $\eta(f)$ from Eq. (2.62) (see also Fig. 2.5**(a)**), even in Case **(C)**, the SSH model does not yield the value of $f_{10} = 3{,}430$ Hz.

(D) Finite locally periodic antisymmetric structure with closed ends
The waveguide corresponding to Case **(D)** is shown in Fig. 2.6**(D)**. The eigenmodes are calculated using Eq. (3.164) and Eq. (3.107), and listed in Tab. 4.6. Compared to the results calculated in Case **(C)**, the SSH approach now yields two more values: $f_1^{\mathrm{D}} = 0$ Hz and $f_{11}^{\mathrm{D}} = 3{,}430$ Hz. Note that f_{11}^{D} corresponds to f_{10} obtained as a root of $\eta(f)$ from Eq. (2.62).

Eigenmode frequency f_i^{C}	Mode type
$f_1^{\mathrm{C}} = 313.51$ Hz	Bulk
$f_2^{\mathrm{C}} = 621.14$ Hz	Bulk
$f_3^{\mathrm{C}} = 911.95$ Hz	Bulk
$f_4^{\mathrm{C}} = 1{,}155.75$ Hz	Bulk
$f_5^{\mathrm{C}} = 1{,}715.00$ Hz	Edge
$f_6^{\mathrm{C}} = 2{,}274.24$ Hz	Bulk
$f_7^{\mathrm{C}} = 2{,}518.05$ Hz	Bulk
$f_8^{\mathrm{C}} = 2{,}808.86$ Hz	Bulk
$f_9^{\mathrm{C}} = 3{,}116.49$ Hz	Bulk

Tab. 4.5: The eigenmodes for Case **(C)**.

Eigenmode frequency f_i^{D}	Mode type
$f_1^{\mathrm{D}} = 0.00$ Hz	Bulk
$f_2^{\mathrm{D}} = 313.51$ Hz	Bulk
$f_3^{\mathrm{D}} = 621.14$ Hz	Bulk
$f_4^{\mathrm{D}} = 911.95$ Hz	Bulk
$f_5^{\mathrm{D}} = 1{,}155.75$ Hz	Bulk
$f_6^{\mathrm{D}} = 1{,}715.00$ Hz	Edge
$f_7^{\mathrm{D}} = 2{,}274.24$ Hz	Bulk
$f_8^{\mathrm{D}} = 2{,}518.05$ Hz	Bulk
$f_9^{\mathrm{D}} = 2{,}808.86$ Hz	Bulk
$f_{10}^{\mathrm{D}} = 3{,}116.49$ Hz	Bulk
$f_{11}^{\mathrm{D}} = 3{,}430.00$ Hz	Bulk

Tab. 4.6: The eigenmodes for Case **(D)**.

The existence of eigenmodes for all four cases is shown in Fig. 4.1. Note that as the value of the coupling coefficient v varies, the number of edge modes changes in addition to the value of the eigenenergies, for Cases **(A)** and **(B)**. Here, there is a transition between bulk and edge modes (and this is where the colour changes). In Cases **(C)** and **(D)**, the eigenmode marked in red represents an edge mode for all values of v. It is also worth noting that the number of eigenmodes is different in each case, which is related to the number of solutions shown in Tabs. 4.3-4.6. In Fig. 4.1, these solutions are represented by cross marks. The band gap boundaries (dashed lines) from Eq. (3.103) delimit the band gap and thus the eigenenergy region of the edge modes.

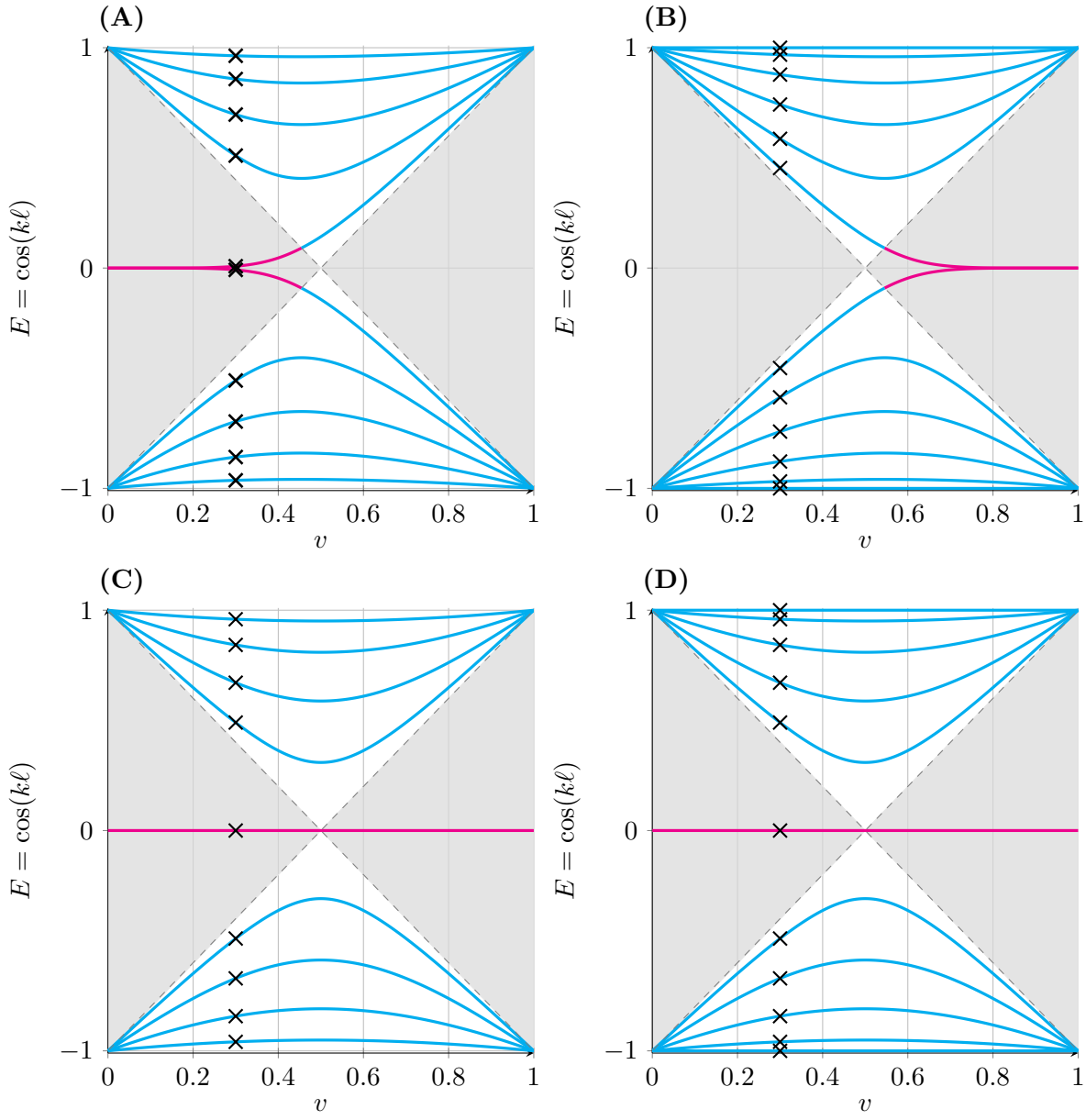

Fig. 4.1: Representation of the existence of eigenmodes through the eigenenergies depending on the value of the coefficient $v \in [0; 1]$. Each curve corresponds to one eigenmode. The edge modes are marked in red. The cross marks correspond to the values calculated in Tabs. 4.3-4.6 and the gray region indicates eigenenergies falling within the band gap.

With the help of the SSH model, we can also easily determine the acoustic pressure amplitudes at discrete positions (in our case, at the edges) of the locally periodic structures. Fig. 4.2 shows the results for the edge mode pressures for Cases **(A)**, **(C)**, and **(D)** according to Eqs. (3.98), (3.144), and (3.160). In Fig. 4.2**(Aa)**, the first edge mode for Case **(A)** is plotted (with antisymmetric amplitudes of pressure) and in **(Ab)**, the second edge mode is plotted (with symmetric amplitudes of pressure). Fig. 4.2**(C)** and **(D)** show the results for a single edge mode.

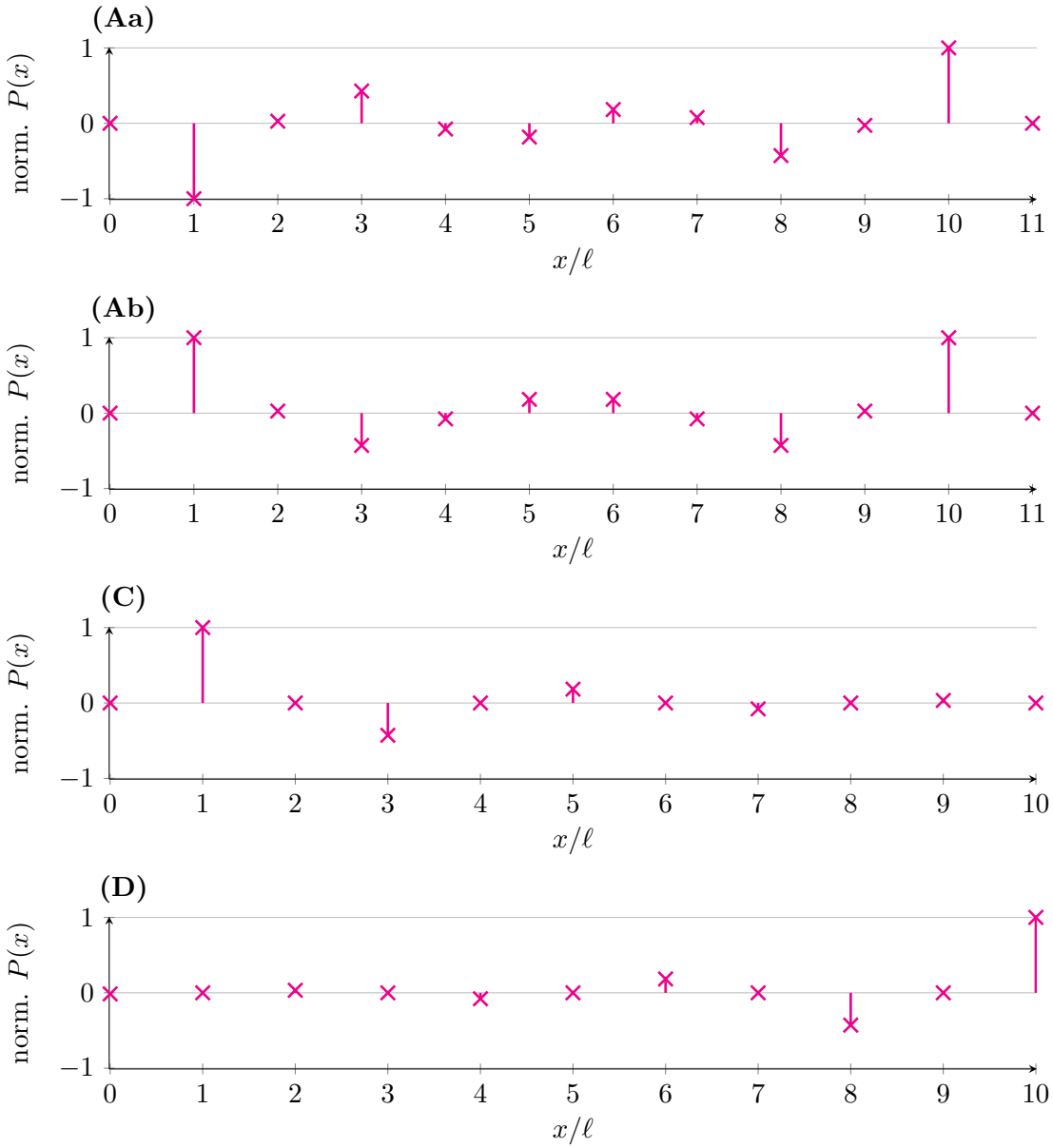

Fig. 4.2: Amplitudes of normalized acoustic pressure for the edge modes at discrete positions of the considered acoustic waveguides are shown. Two edge modes from Case **(A)** correspond to **(Aa)** and **(Ab)**, and Cases **(C)** and **(D)** to **(C)** and **(D)**, respectively.

Chapter 5

Discussion

In the context of the thesis, the impact of boundary conditions on the existence of edge modes was clearly demonstrated. We have shown the application of the one-dimensional discrete SSH model to locally periodic structures with different terminations and also depending on the variable ratio of the cross-sectional areas of alternating elements.
The TMM, a traditionally used approach, helped us verify the frequency and transmission properties of acoustic waveguides obtained in the SSH analysis. However, using the transfer matrix for more complex systems requires a more complex adaptation, both for assembling the matrix itself and for calculating the roots of functional expressions that arise from the boundary conditions.
The SSH model, a more versatile approach not widely used in acoustics, remains unchanged with different waveguide structures, allowing edge modes to be predicted in this manner. An advantage of the SSH model is also its easier scalability to 2D cases [23]. It turns out that the approach using the SSH model is much easier for calculating eigenfrequencies and also amplitudes of acoustic pressure at discrete positions of the considered waveguides based on boundary conditions, unlike the TMM. The SSH model also provides more information about whether edge modes can occur in the given structure.
The existence of edge modes was experimentally confirmed (as presented in [11]), with analytical calculations, experiments, and simulations showing good agreement. The article further demonstrated the topological robustness against disorders, also verified experimentally. According to the authors, these findings apply to the 2D case as well [23].
With increasing frequency within the plane wave approximation, discrepancies arise in locations with step changes in cross-section (again, see [11]), leading to deviations where the approximation no longer holds, and the waves are not plane. This primarily concerns higher frequencies (from half of the interval $f \in (0; f_c)$). For lower frequencies (from the first half of the mentioned interval), the approximation is satisfactory. However, in cases where $v \approx 0.5$ (near the point where the bandgap closes), the approximation is very suitable, and for $v = w$, it aligns with theory.

As demonstrated in the previous chapters, edge modes appear in finite (locally periodic) structures; however, their existence also depends on the ratio of the coupling coefficients v and w in some cases (this is clearly illustrated in Fig. 4.1). In the previous chapters, we focused exclusively on waveguides with symmetric boundary conditions, meaning that both ends were either open or closed (always starting with a cross-sectional area denoted by S_B). It is also possible to analyse antisymmetric terminations of structures (i.e., partially open waveguides), but these cases are not detailed in this thesis because of its required extent. However, in Tab. 5.1, we show how the symmetry of the structure itself and the symmetry of the boundary conditions relate to the existence of eigenmodes, depending on the ratio of the coupling coefficients. Note that even within the interval $v < w$ or $v > w$, the number of edge modes can vary. This is demonstrated,

for instance, in Case **(A)** in Section 3.3 and also in Figs. 4.1**(A)** and **(B)**.
The values in Tab. 5.1 are based on the calculations from Chapter 4, using the same waveguide parameters as those listed in Tab. 4.1.

Waveguide Case	Waveguide Symmetry	Boundary Conditions (Left End, Right End)	Edge Modes Number for $v < w$	Edge Modes Number for $v > w$
(A)	Symmetric	Open, Open	2 or 0	0
(B)	Symmetric	Closed, Closed	0	0 or 2
(C)	Antisymmetric	Open, Open	1	1
(D)	Antisymmetric	Closed, Closed	1	1
-	Symmetric	Open, Closed	1	1
-	Symmetric	Closed, Open	1	1
-	Antisymmetric	Open, Closed	2 or 0	0
-	Antisymmetric	Closed, Open	0	0 or 2

Tab. 5.1: The relationship between symmetric and antisymmetric configurations of the boundary conditions and the existence of eigenmodes based on the ratio of the coupling coefficients v and w for specific acoustic waveguides.

Chapter 6

Conclusion

In this thesis, we focused on investigating the resonant, dispersive, and transmission properties of selected locally periodic binary acoustic waveguides. We also discussed the significance of the Bloch-Floquet theory and selected concepts from topological acoustics. The analysis was conducted using the TMM and the one-dimensional SSH model, which became an alternative approach not typically used in acoustics. Comparing both methods allowed us to evaluate the results for the studied finite locally periodic structures with specific boundary conditions crucial for the existence of edge modes. In several cases, we performed an analysis of eigenmodes and then calculated numerical values for the waveguides with selected parameters. In Discussion, we commented on the contributions and shortcomings of each method as well as placing the issues studied in a broader context with reference to further scientific work. Selected symbolic derivations and numerical calculations using Maple software were also included as an attachment to this thesis.
All the requirements of the bachelor's thesis have been met.

Bibliography

[1] A. Coutant, V. Achilleos, O. Richoux, G. Theocharis, and V. Pagneux. Subwavelength Su-Schrieffer-Heeger topological modes in acoustic waveguides. The Journal of the Acoustical Society of America, 151(6):3626–3632, June 2022. ISSN 1520-8524. doi: 10.1121/10.0011550.

[2] X. Li, Y. Meng, X. Wu, S. Yan, Y. Huang, S. Wang, and W. Wen. Su-Schrieffer-Heeger model inspired acoustic interface states and edge states. Applied Physics Letters, 113(20), November 2018. ISSN 1077-3118. doi: 10.1063/1.5051523.

[3] A. Rajabpoor Alisepahi, S. Sarkar, K. Sun, and J. Ma. Breakdown of conventional winding number calculation in one-dimensional lattices with interactions beyond nearest neighbors. Communications Physics, 6(1), November 2023. ISSN 2399-3650. doi: 10.1038/s42005-023-01461-0.

[4] A. Anastasiadis, G. Styliaris, R. Chaunsali, G. Theocharis, and F. K. Diakonos. Bulk-edge correspondence in the trimer Su-Schrieffer-Heeger model. Physical Review B, 106(8), August 2022. ISSN 2469-9969. doi: 10.1103/physrevb.106.085109.

[5] P. Delplace, D. Ullmo, and G. Montambaux. Zak phase and the existence of edge states in graphene. Physical Review B, 84(19), November 2011. ISSN 1550-235X. doi: 10.1103/physrevb.84.195452.

[6] J. K. Asbóth, L. Oroszlány, and A. Pályi. A Short Course on Topological Insulators: Band-structure topology and edge states in one and two dimensions. arXiv, 2015. ISBN 9783319256054.

[7] G. Ma, M. Xiao, and C. T. Chan. Topological phases in acoustic and mechanical systems. Nature Reviews Physics, 1(4):281–294, March 2019. ISSN 2522-5820. doi: 10.1038/s42254-019-0030-x.

[8] P. Markos and C. M. Soukoulis. Wave Propagation: From Electrons to Photonic Crystals and Left-Handed Materials. Princeton University Press, 2008. ISBN 9780691130033.

[9] Z. Fu, N. Fu, H. Zhang, Z. Wang, D. Zhao, and S. Ke. Extended SSH Model in Non-Hermitian Waveguides with Alternating Real and Imaginary Couplings. Applied Sciences, 10(10):3425, May 2020. ISSN 2076-3417. doi: 10.3390/app10103425.

[10] Y.-X. Shen, L.-S. Zeng, Z.-G. Geng, D.-G. Zhao, Y.-G. Peng, and X.-F. Zhu. Acoustic Adiabatic Propagation Based on Topological Pumping in a Coupled Multicavity Chain Lattice. Physical Review Applied, 14(1), July 2020. ISSN 2331-7019. doi: 10.1103/physrevapplied.14.014043.

[11] A. Coutant, A. Sivadon, L. Zheng, V. Achilleos, O. Richoux, G. Theocharis, and V. Pagneux. Acoustic Su-Schrieffer-Heeger lattice: Direct mapping of acoustic waveguides to the Su-Schrieffer-Heeger model. Physical Review B, 103(22), June 2021. ISSN 2469-9969. doi: 10.1103/physrevb.103.224309.

[12] X. Huang, J. Lu, W. Deng, and Z. Liu. Topological materials for elastic wave in continuum. Acta Mechanica Sinica, 39(7), June 2023. ISSN 1614-3116. doi: 10.1007/s10409-023-23041-x.

[13] H. Jiang, W. Liu, J. Xu, B. Gao, C. Zhu, S. Xie, and Y. Yang. Topological edge modes in one-dimensional photonic crystals containing metal. OSA Continuum, 4(5):1626, May 2021. ISSN 2578-7519. doi: 10.1364/osac.416906.

[14] L. Thatcher, P. Fairfield, L. Merlo-Ramírez, and J. M. Merlo. Experimental observation of topological phase transitions in a mechanical 1D-SSH model. Physica Scripta, 97(3):035702, February 2022. ISSN 1402-4896. doi: 10.1088/1402-4896/ac4ed2.

[15] K. Yatsugi, T. Yoshida, T. Mizoguchi, Y. Kuno, H. Iizuka, Y. Tadokoro, and Y. Hatsugai. Observation of bulk-edge correspondence in topological pumping based on a tunable electric circuit. Communications Physics, 5(1), July 2022. ISSN 2399-3650. doi: 10.1038/s42005-022-00957-5.

[16] S. M. Kuznetsova, J.-P. Groby, L. M. García-Raffi, and V. Romero-García. Localized interface modes in one-dimensional hyperuniform acoustic materials. Journal of Physics D: Applied Physics, 54(31):315303, May 2021. ISSN 1361-6463. doi: 10.1088/1361-6463/ac006d.

[17] M. Padlewski, M. Volery, R. Fleury, H. Lissek, and X. Guo. Active Acoustic Su-Schrieffer-Heeger-Like Metamaterial. Physical Review Applied, 20(1), July 2023. ISSN 2331-7019. doi: 10.1103/physrevapplied.20.014022.

[18] M. Bednařík and M. Červenka. Propagation of electromagnetic waves through non-uniform dielectric layers. Journal of the Optical Society of America B, 35(10):2541, September 2018. ISSN 1520-8540. doi: 10.1364/josab.35.002541.

[19] M. L. Munjal. Acoustics of Ducts and Mufflers. Wiley, Location of Publisher, 2014. ISBN 9781118443125.

[20] D. J. Griffiths and C. A. Steinke. Waves in locally periodic media. American Journal of Physics, 69(2):137–154, February 2001. ISSN 1943-2909. doi: 10.1119/1.1308266.

[21] S. Lang. Linear Algebra. Springer, New York, 3rd edition, 1987. ISBN 9780387964126.

[22] K. F. Riley, M. P. Hobson, and S. J. Bence. Mathematical Methods for Physics and Engineering. Cambridge University Press, 2006. ISBN 9780511810763.

[23] A. Coutant, V. Achilleos, O. Richoux, G. Theocharis, and V. Pagneux. Topological two-dimensional Su–Schrieffer–Heeger analog acoustic networks: Total reflection at corners and corner induced modes. Journal of Applied Physics, 129(12), March 2021. ISSN 1089-7550. doi: 10.1063/5.0042406.

Appendix A

Attached CD Contents

The following scripts contain selected symbolic derivations of the theoretical relationships presented in this thesis, as well as some of the numerical calculations. These files can be used for verification or subsequent related work:

- `tmm_derivations.mw` for Chapter 2,
- `tmm_calculations.mw` for Chapters 2 and 4,
- `ssh_derivations.mw` for Chapter 3,
- `ssh_calculations.mw` for Chapters 3 and 4.

An electronic version of this bachelor's thesis is also attached:

- `thesis_body.pdf`.